

**“Babeş-Bolyai” University**  
**Faculty of Physics**

**Spectroscopic and electric investigations of some polymers  
of general use**

**Summary**

**Scientific Supervisor:**

**Prof. Univ. PhD Todică Mihai**

**PhD Student:**

**Ştefan Traian**

**Cluj-Napoca**

**2013**

## Table of contents

<b><i>Introduction</i></b>	<b>3</b>
<b><i>I. Polymeric Membranes</i></b>	<b>5</b>
1.1 <i>Polymeric Membranes and Applications</i>	5
1.2 <i>Applications of polyvinyl alcohol (PVA) and polyacrylic acid (PAA) in the pharmaceutical industry and technology of fuel cells</i>	9
1.3 <i>Techniques for obtaining polymeric membranes</i>	12
<b><i>II. Study methods and apparatus used</i></b>	<b>15</b>
2.1 <i>Electrical measurements</i>	15
2.2 <i>UV-VIS Spectroscopy</i>	19
2.3 <i>IR spectroscopy</i>	23
2.4 <i>Raman Spectroscopy</i>	26
2.5 <i>Electron spin resonance spectroscopy (EPR)</i>	33
2.6 <i>X-ray diffraction spectroscopy</i>	35
2.7 <i>Differential thermal calorimetry (DSC)</i>	41
<b><i>III. Experimental results</i></b>	<b>43</b>
3.1 <i>Preparation of membranes</i>	43
3.2 <i>Electrical Investigations</i>	46
3.2.1 <i>Electrical resistivity measurements</i>	46
3.2.2 <i>Determination of dielectric permittivity</i>	59
3.3 <i>Spectroscopic Investigation of PVA membranes doped with TiO<sub>2</sub></i>	71
3.3.1 <i>UV-VIS Investigation</i>	71
3.3.2 <i>Raman Investigation</i>	75
3.3.3 <i>Investigation by EPR</i>	80
3.3.4 <i>X-ray diffraction investigations</i>	84
3.3.5 <i>DSC investigation of PVA membranes doped with TiO<sub>2</sub></i>	93
3.4 <i>Spectroscopic Investigation of pure and carbon doped PVA membranes</i>	97
3.4.1 <i>IR Investigation of pure and carbon doped PVA membranes</i>	97

3.4.2 <i>UV-VIS Investigation</i>	101
3.4.3. <i>Raman Investigation</i>	104
3.4.4. <i>XRD Investigation</i>	108
3.4.5 <i>EPR Investigation of carbon doped PVA membranes</i>	110
<b><i>IV. Polymeric fuel cell electrode</i></b>	<b>114</b>
4.1 <i>Use of PVA membranes doped with TiO<sub>2</sub> and carbon in fuel cells engine</i>	114
4.2 <i>Fuel Cells</i>	115
4.3 <i>Functional Principles</i>	115
4.4 <i>Testing PVA polymer membranes for D.M.F.C construction</i>	118
<b><i>V. Spectroscopic Investigation of PAA membranes</i></b>	<b>124</b>
5.1 <i>Spectroscopic Investigation of carbon-doped PAA membranes</i>	124
5.1.1 <i>UV-VIS Investigation</i>	124
5.1.2. <i>XRD Investigation</i>	126
5.1.3 <i>EPR Investigation of Carbon doped PAA membranes</i>	134
5.2 <i>Spectroscopic Investigation of TiO<sub>2</sub> doped PAA membranes</i>	140
5.2.1. <i>UV-VIS Investigations</i>	141
5.2.2 <i>Raman Investigations</i>	144
<b><i>General conclusions</i></b>	<b>149</b>

***Keywords:***

Polyvinyl alcohol, polyacrylic acid, carbon, titanium dioxide, methanol, polymers, monomers, gels, membranes, polymer electrodes, fuel cells, resistivity, permittivity, radiation, Raman, electron paramagnetic resonance, X-ray diffraction

## **Introduction**

The synthetic polymers represent over two thirds of the global chemical industry. Almost half of the objects handled daily by humans are polymers or are containing polymers. These findings suggest the importance that polymers have gained in the actual world. They greatly expanded the range of useful materials for the modern man, which justifies the research efforts aiming the complex study of these types of artificial materials.

After 1965, when the German chemist Karl Ziegler succeeded the polymerization at moderate temperatures and pressures by means of polymerization catalysts, the polymer industry has gained a great extent, becoming among the most important branches of chemical industry. Polymers can offer various material structures from micrometre-sized fibres and membranes to compact and durable objects that, unlike compact mineral or metallic structures, have the advantage that they can reach densities lower than the density of water, preserving reasonable mechanical qualities. This is due to the remarkable properties of the carbon atom (a chemical element with relatively small mass) to easily form strong covalent bonds with itself and with many other elements forming macromolecules (there are known over two million chemical species that have the common integrative element the carbon's covalences).

The natural polymers as well as those from the structure of living matter (biopolymers) have emerged with the synthesis of organic matter and they are underlying life. Simultaneously combining the properties of solids and viscous liquids, the polymers are often able to offer unique and optimal solutions in many practical situations [1].

In this thesis, I have presented the results of electrical and spectroscopic investigations carried out on membranes containing pure or combined with additives

polymers, seeking possible changes of some electrical properties and microscopic structural changes occurred after contamination.

Since in some applications, primarily in the medico-pharmaceutical field, the polymers can be intentionally or accidentally exposed to gamma irradiation processes (e.g. during sterilization procedures or specific therapeutic manoeuvres), I have seek electrical or spectroscopic behaviour changes occurred after irradiation.

The polymers used were PVA (polyvinyl alcohol) and PAA (polyacrylic acid) and the predominantly added dopants were black carbon powder and titanium dioxide. It was also studied the possibility of using membranes made of PVA doped with carbon and, respectively, titanium dioxide, at the construction of basic fuel cells using methanol as fuel. In the performed experiments, I have resorted to gamma irradiation of these membranes in order to establish if any structural changes induced by radiation could be useful to the proposed application. The work was divided into two parts. The first part is devoted to the description of the overall polymer membranes, their general properties and methods of the investigation, and the second part contains the experimental results obtained and the conclusions drawn from the experiments.

## **CHAPTER 1. Polymeric membranes**

This chapter presents a definition of the polymer membrane taking into account the morphological and functional criteria, exhibits a classification of types of membranes used in various applications, shows modern technological methods of obtaining these membranes, as well as specific applications of polyvinyl alcohol and polyacrylic acid in pharmacology, in the construction of sensors or electric fuel cells. The entire work is devoted to the study of these two polymers, in pure form or contaminated with inorganic powders and also after exposure to different doses of gamma radiation.

### **1.1 Polymeric membranes and applications**

Polymers are a class of substances composed of macromolecules formed by chaining covalent bonds of  $n$  identical units called monomers. Many polymers have good elastic properties and can be processed into thin foils (flexible membranes) or have the

property that, under the action of some solvents, to physically absorb solvent molecules becoming soft and forming gels. By solvent evaporation, the gel becomes solid again and this facilitates the obtaining of membranes by simply stretching a layer on a plane support and then leaving it to dry. The membrane is a selective barrier that actively or passively participates in mass transfer between phases that separate them.

## **1. Superacidic membranes**

Besides common types of membranes used widely as separators where there is actually a transfer of substances between compartments bounded by membranes through various mechanisms (capillary pressure gradients, concentration, apparent dissolution of the membrane in the work environment), there were recently created membranes, almost impermeable to molecules of separated chemical species, which still allow the easy transfer of the proton ( $H^+$ ) in the sense determined by the electrochemical potential gradient. They are made of doped polymeric compounds and they have hydrogen atoms which are weakly bounded to the skeleton of the molecule. This vulnerable link may arise between a hydrogen atom and an O atom of an OH marginal group, where doping a polymer with a very electronegative dopant (e.g. F1 of Nafion). Weak links can be induced also by neutral dopants which, by interposing themselves between the macromolecules of the polymer matrix, determine conformational changes by disrupting the pre-existing electrostatic equilibrium, so that some hydrogen atoms bounded to electronegative elements (e.g. O) get in the position of weakly bounded atoms (this is the PVA case, doped with  $TiO_2$  and studied here).

### **1.2 Applications of polyvinyl alcohol (PVA) and polyacrylic acid (PAA) in pharmaceutical industry and in the technology of fuel cells**

This thesis aimed to study the PVA and PAA polymers, pure and doped with inorganic nanoparticles, (mainly  $TiO_2$  and carbon). These polymers of simple monomeric structure are extensively used in various applications, both in gel form as well as thin membranes or as compact polymer mass.

The study was performed on the same polymer after gamma irradiation with different doses up to 17 KGy, in order to observe changes, induced by radiation, in the structure and electrical properties. The PVA membranes doped with TiO<sub>2</sub> are used in technique as solid electrolytes in proton exchange fuel cells. After doping with carbon nanoparticles, they can be used as electrode catalysts in the manufacture of polymer fuel cells. In the pharmaceutical industry, PVA can be used to support various drug substances, being biocompatible.

The polyacrylic acid (PAA) also has applications in pharmacology, to support active drug substances and it is biocompatible. The polymer matrix can embed into its structure medicinal substances and then gradually release them as slow dissolution of the polymer, thus extending the period of action of the drug on diseased tissue. The process is mostly applied in dermatological treatments, the substances being applied on the skin and on mucous membranes. The exposure to high doses of gamma radiation sterilization is commonly used, sometimes as a method of therapy for skin diseases and neoplasms. Such high-energy radiation can induce degradation of the polymer matrix by ionizing atoms, breaking molecular bonds with chain scission, followed by changes in physical properties such as UV-VIS transparency or crystallinity. The knowledge of the effect induced by irradiation on polymer matrix and the knowledge of the maximum dose tolerated by the product before degradation are of interest for medical use. These possible changes in the polymer substrate after exposure to gamma radiation are not well known, so, there is a need to be carried out experiments and investigations to elucidate some aspects of this process.

Observations can be made at microscopic scale by UV-VIS spectroscopic techniques, IR, Raman, EPR and XRD. At the macro scale, we can get useful information by appealing to electrical resistivity and dielectric permittivity measurements.

## **CHAPTER 2. Study methods and apparatus used**

This section shows the types of investigations that were used for deciphering the macroscopic and microscopic physical properties of the samples proposed for study, as well as the laboratory equipment used to achieve these objectives. There were performed

mainly electrical resistivity and permittivity measurements and UV-VIS spectroscopic investigations, IR, Raman, XRD, EPR spectrometry or thermal investigations (DSC).

Such investigations were differentially carried on categories of samples, according to the intended purpose and the alleged value of the information provided by them, in the context of particular practical applications concerned here.

## **2.1 Electrical Measurements**

The electrical measurements provide information about the behaviour of polymers placed in electric field or exposed to potential differences. It can be highlighted such molecular properties as polarizability and mobility of charge overall carriers. These measurements are important in terms of practical application on polymer technique.

### **A. Determining resistivity**

Pure polymers are characterized by high electrical resistivity, which is necessary to be measured by special methods or by direct measurement using a teraohmmeter. The teraohmmeter allows a direct measurement of high resistivity values using analogue or digital display. The Orion TR -2201 teraohmmeter used here has the maximal domain  $50 \times 10^7 \text{ M}\Omega$  and enables to apply a continuous voltage between 0-1000 V, in steps of 100V, on the sample.

### **B. Determination of dielectric permittivity**

Permittivity is an important feature of the polymeric materials and its knowledge is important for practical applications, e.g. in electronics and sensor construction.

To determine the permittivity, we used a Tesla BM409 Q-meter, which allows assessing the permittivity variation by frequency, in a method that is based on the appearance of resonance in RLC circuits (Fig.2.2).

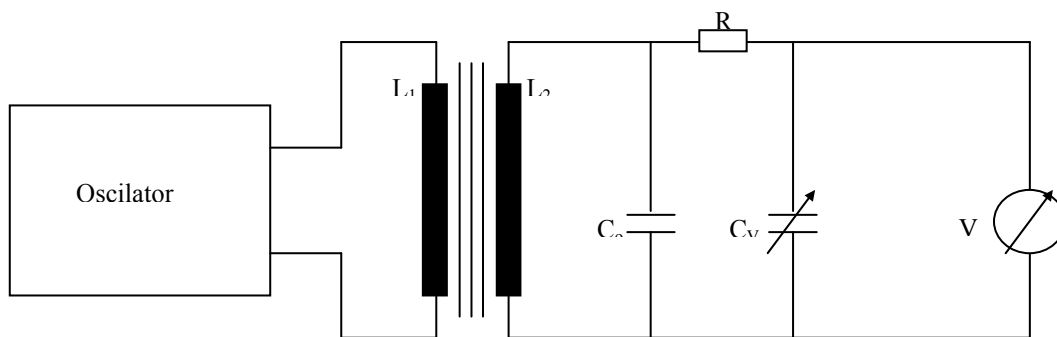


Fig. 2.2. The schematic diagram of the experimental setup used to measure the dielectric constant by resonance method.

## 1.2 Spectroscopic Investigation

The UV-VIS investigations were made using a Jasco V-670 system, with a scan speed of 200 nm / min, UV-VIS bandwidth of 2 nm, and NIR bandwidth of 8 nm.

The IR investigations were carried out on an Equinox 55 spectrometer, FT-IR type.

The Raman spectra were recorded with the WITEC CRM 200 equipment, a confocal Raman microscope, at room temperature. All Raman spectra were obtained by exciting the samples with light produced by a 100 mW He-Ne laser with a wavelength of 633 nm.

The EPR spectra presented in this paper were recorded at room temperature with Bruker - BioSpin EMX spectrometer, operating in X-band (9-10 GHz).

The X-ray diffraction (XRD) was done with Bruker X-ray diffractometer with Cu Ka ( $\lambda = 0154$  nm) at 45 kV and 40 mA. It was recorded all the  $2\theta$  angular range between 10-120°.

The differential thermal analysis measurements were performed with Shimadzu thermal equipment, DTG 60/60 H.

The exposure to gamma radiation of the membranes was performed using  $^{60}\text{Co}$  sources with 5 Gy radiation flow/h during different time intervals, to the maximum dose of 17 KGy.



Figure 2.11. The photo of the oven used to perform DSC.

### **CHAPTER 3. Experimental results**

This chapter discusses the experimental results obtained from electrical, thermal and spectroscopic investigations performed on the prepared samples. The electrical investigations were performed on batches of PAA and PVA samples, in order to highlight the similarities and peculiarities of parameters belonging to each type of polymer.

The spectroscopic investigations presented in this chapter refer only to samples that were used in practical applications.

#### **3.1 Preparation of membranes**

In experiments, we especially used polyvinyl alcohol (PVA), poly-acrylic acid, (PAA), pure and doped with inorganic substances of which the most used are  $\text{TiO}_2$  and carbon.

The polyvinyl alcohol (PVA) with monomer  $\text{C}_2\text{H}_3\text{O}$  (Photo.1) and the polyacrylic acid (PAA) with monomer (  $\text{CH}_2$  -CH-  $\text{COOH}$ ) are in the form of white powder with specific gravity of  $1.293 \text{ g/cm}^3$ , for PVA, and  $1.320 \text{ g/cm}^3$ , for PAA. Both substances are hygroscopic and highly soluble in distilled water, at room temperature, water dissolving up to a concentration of 30% mass of polymer, forming a transparent gel with the consistency depending on the variable percentage of water used as solvent. Polyvinyl

alcohol is insoluble in pure methanol as well as in its concentrated solution with water. In order to ensure a good homogeneity and a uniform dispersion, we used a doping concentration of 10% polymer. The membranes were prepared from pure polymer, dissolved in distilled water and then stir vigorously, and eventually, ultrasonic. The low consistency transparent gel obtained is spread on a support plane for drying outdoors. If you want to obtain membranes with higher thickness, the dryness can be made in vats equipped with flat edges.

For experiment some fuel cells, PVA membranes doped with carbon have been made with a thickness greater than 1 mm, in order to give a considerable volume of absorbent for the reaction. Drying at ventilated room temperature lasts about 48 hours, and it is longer for thicker membranes. The obtained membranes are transparent, flexible for PVA and the PAA is stiffer and more brittle. The membranes doped with carbon has been obtained from an aqueous gel, which is added to the natural carbon (Aldrich origin is presented in the form of fine black nanoparticles) of purity 99.9% to the desired concentration (1%, 5%, 15%, 30% and 50%) compared to the mass of PVA or PAA, (Photo.2).

The membrane's porosity increases progressively with the addition of carbon but above a 50% carbon, the binding role of PVA or PAA membranes disappears and crumbles. The  $\text{TiO}_2$  doping is achieved as well as carbon doping.  $\text{TiO}_2$  is used in the form of white nanoparticles (predominantly anatase phase) and has a purity of 99.5%.

After doping with  $\text{TiO}_2$ , there were obtained white membranes with variable transparency by the proportion of  $\text{TiO}_2$  added. At 50%  $\text{TiO}_2$ , the membranes are opaque to visible light. After doping with carbon, the membranes became opaque at 30% black carbon.



Photo.1. The PVA monomer and its presentation form before preparing membranes.



Photo.2. The image of black carbon

The drying of the membranes was thoroughly followed, in order to know the amount of water remaining in the final polymer matrix component, (water related) that influence the electrical parameter values of the spectroscopic behaviour of the samples (Fig.3.1).

It was found that the mass of dry membrane is greater than the mass of powder originally used in the preparation of the membrane, which indicates that membrane molecules permanently retain water as bound water. Thus, the difference between the mass of the PAA membrane and the initial PAA powder is  $0.2960 - 0.2800 \text{ g} = 0.016 \text{ g}$ , and for PVA, the difference is  $1.3025 - 1.2800 = 0.0225 \text{ g}$ , the water left representing approximately 5 w% , for PAA, respectively, 2 w%, for PVA..

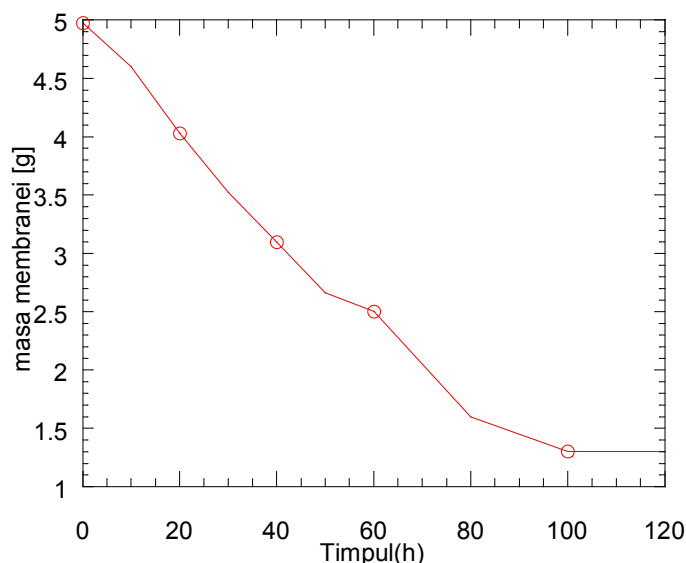


Fig . 3.1. The PVA membrane. The weight is presented according to the drying time

## 3.2. Electrical Investigations

### 3.2.1. Measurements of electrical resistivity

The knowledge of electrical resistivity is of interest for applications in technical polymers. For example, for use as dielectrics in capacitors manufacture as electrical insulators or as solid electrolytes in fuel cells must present a high resistivity. In exchange for building polymer electrodes fuel cells must submit minimum resistivity. For use as gas sensors must be the dependent variable resistivity of gas absorption. The vast majority of polymers are characterized by very low electrical conductivity. One way to achieve electrical conduction in the polymer is to introduce their inorganic elements in the matrix. This achieves a composite material in which there is chemical bond between the polymer and dopant, the dopant is present in the premises caused by imperfect packing of polymer chains that binds physical weaknesses. The polymer itself does not participate in the transfer duties scarcely electrical conductivity is determined almost exclusively by the dopant. The conductivity of the composite is determined by the connectivity that exists between the spatial domains occupied by the dopant. The

interaction of gamma radiation with polymer chains may result in excitation of atoms, splitting or breaking of links polymer chains of the monomers, followed by the appearance of ions and free electrons. Chain scission leads to local segmental dynamics, followed by changing polymer network. In this case, the probability of establishing connections between the areas occupied by the dopant increases, being followed by increased electrical conductivity.

Resistivity measurements showed generally increasing resistivity samples irradiated PAA or PVA gel as water evaporation, ( Fig.3.2 ) after doping with  $\text{TiO}_2$  ( Fig. 3.3 ) or sulphur ( Table 3.1) and its sharp decrease after doping with carbon (Table 3.2).

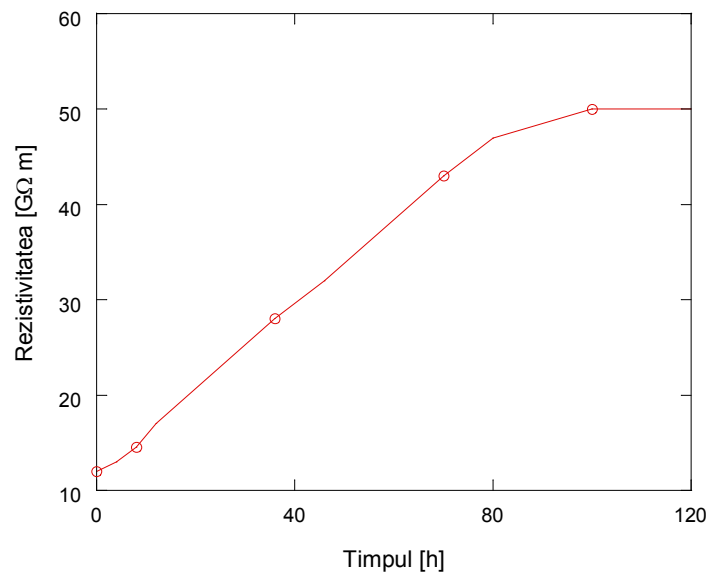


Fig.3.2 . The PAA membrane. The resistivity is presented according to the drying time.

Table 3.1 Resistivity of PAA membranes doped with sulphur.

Polymer type	Doping percentage %	Resistivity GΩm
Pure PAA	0	50
PAA-S	5	80
PAA-S	10	135
PAA-S	15	160
PAA-S	30	230

Table 3.2. The carbon doped PVA membranes resistivity by doping percentage.

Carbon doped PVA membrane	Doping level	Resistivity after 1 day of drying	Resistivity after 7 days
Pure PVA	0%	1600 GΩm	2000 GΩm
PVA-C	50%	460 Ωm	230 Ωm
PVA-C	5%	4100Ωm	2800 Ωm
PVA-C	15%	1470 Ωm	1120 Ωm
PVA-C	30%	800 Ωm	560 Ωm

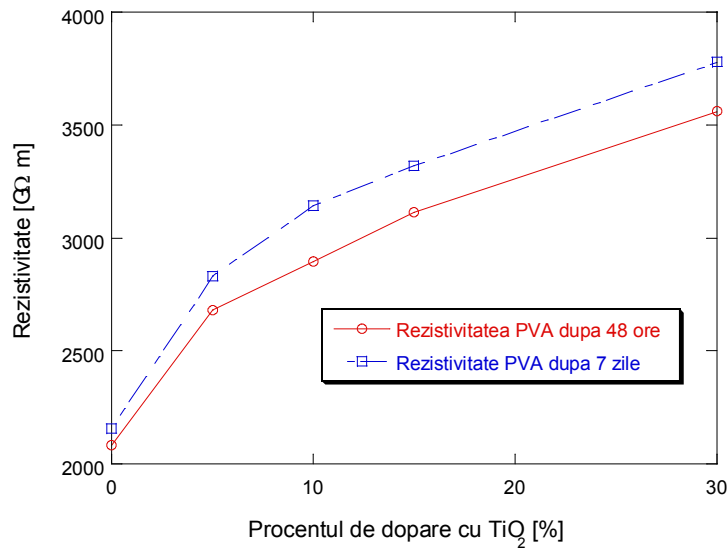


Figure 3.3. The resistivity of partially and completely dried PVA membrane according to the TiO<sub>2</sub> doping percentage.

The PVA and PAA membranes of pure and doped TiO<sub>2</sub> (Fig.3.4) and carbon (Fig.3.5) were subjected to gamma irradiation, to observe any effects exerted by these penetrating radiation, effects which are detectable by measuring the electrical resistivity. Thus, decreasing trend of the resistivity has been observed, following the action of the radioactive radiation.

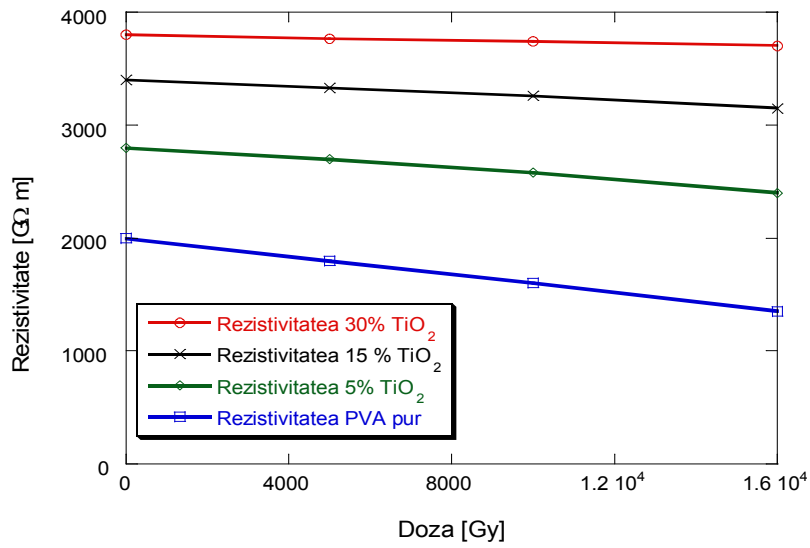


Fig. 3.4 The resistivity of pure and TiO<sub>2</sub> doped (5.15 and 30%) PVA membrane depending on the cumulative gamma dose.

Measurements were performed after irradiation with doses of 5000, 10000 or 16000 Gy found a continuous decrease of the resistivity with dose accumulation.

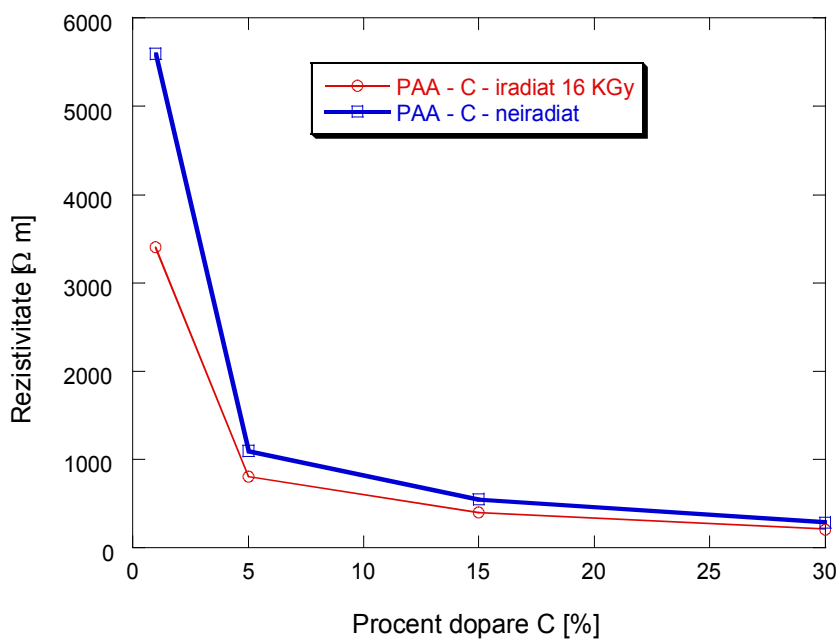


Fig. 3.5. The resistivity of PAA-C gamma irradiated (16 KGy) and non-irradiated according to the percentage of doping.

### Determination of dielectric permittivity

We performed measurements to observe the influence of permittivity of free water, the frequency of doping and gamma irradiation on the dielectric constant of polymers. We found that the permittivity increases free water samples (Fig.3.6). Increased frequency external electric field leads to consistently lower permittivity. (Figure 3.7).

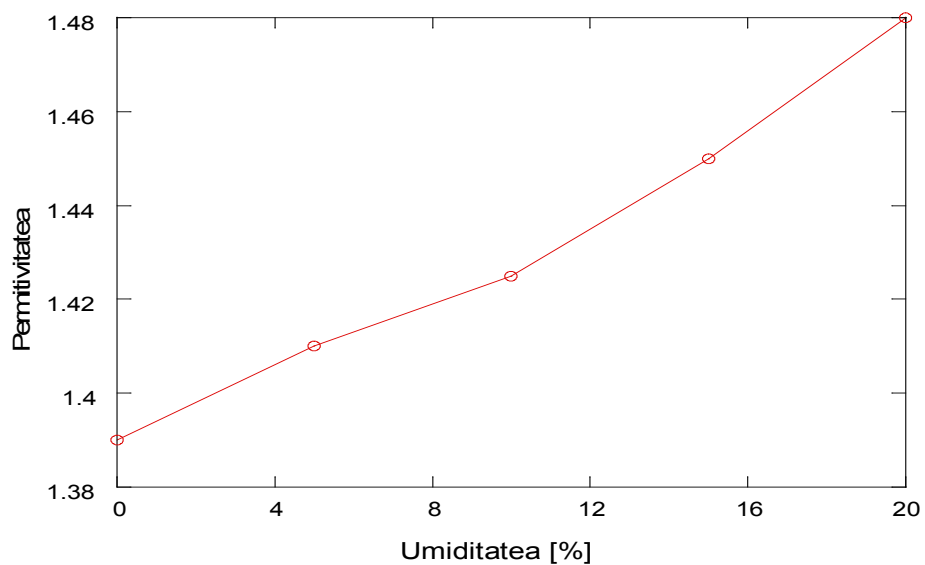


Fig. 3.6. The pure PVA sample's permittivity depending on humidity.

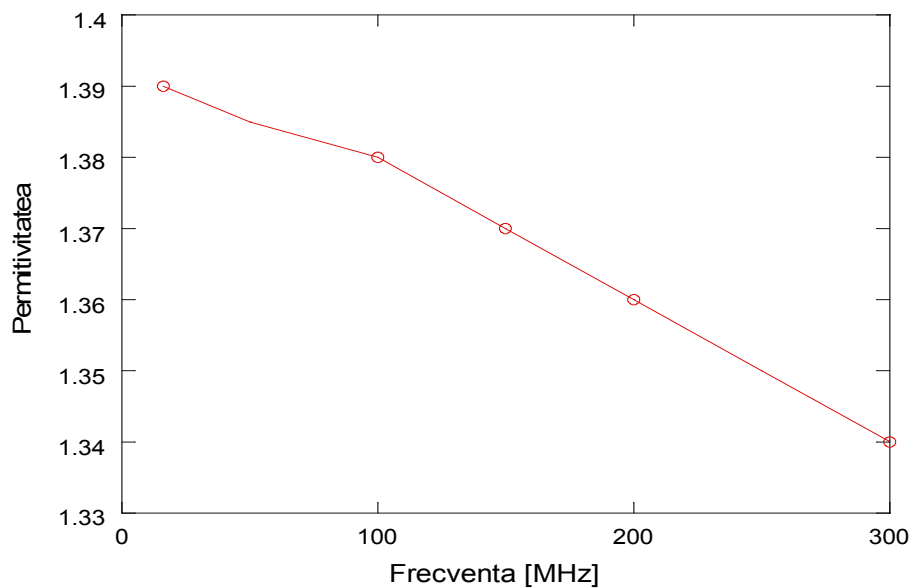


Fig. 3.7. The pure PVA sample's permittivity depending on frequency.

Penetration of  $\text{TiO}_2$  (Fig.3.8) or carbon (Fig.3.9) also causes lower permittivity.

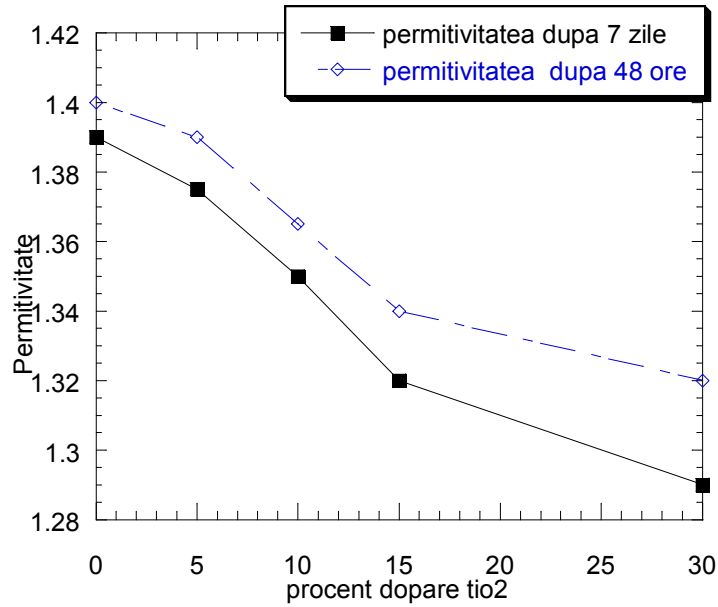


Fig.3.8 The PVA membrane's permittivity, completely dried and semi dried, according to the  $\text{TiO}_2$  percentage of doping.

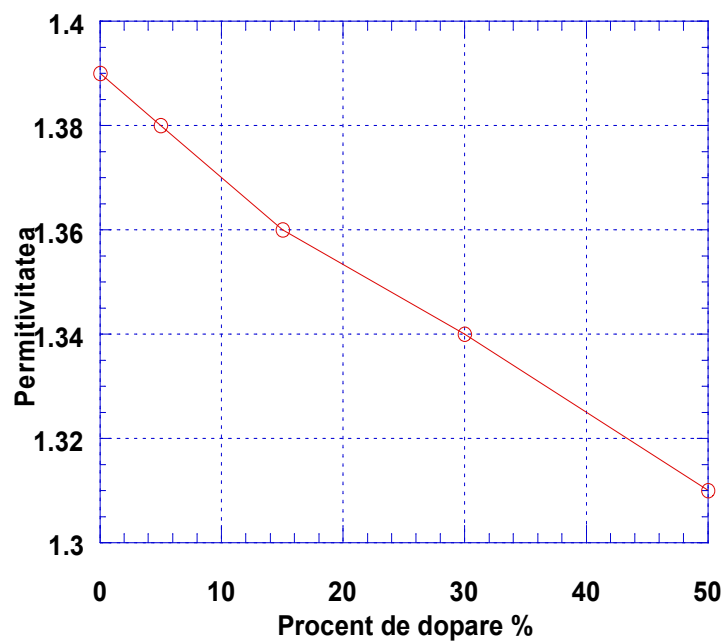


Fig.3.9 The carbon doped PVA membrane's permittivity according to the percentage of doping.

After gamma irradiation is found slight increase in permittivity both pure samples and for the most contaminated with  $\text{TiO}_2$  (Fig.3.27) or carbon (Fig 3.29.)

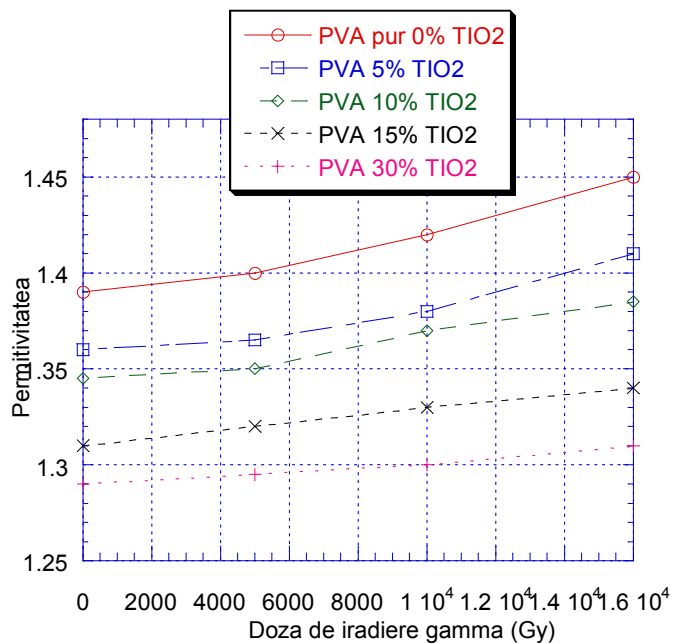


Figure 3.27. The permittivity of pure and TiO<sub>2</sub>doped PVA membranes by gamma irradiation dose.

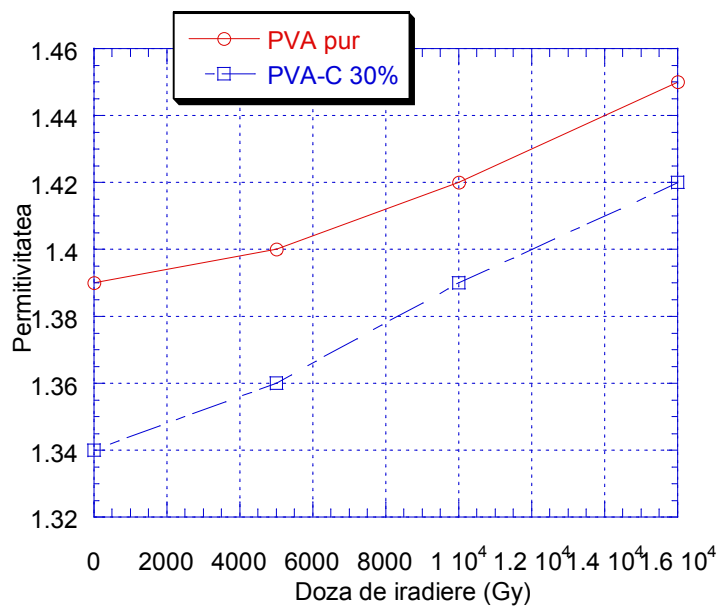


Fig. 3.29 The doped with 30% carbon PVA membranes' permittivity by gamma irradiation dose.

### 3.3. Spectroscopic Investigation of pure and doped PVA membranes with TiO<sub>2</sub>

For pure PVA sample, the absorption maximum is observed at 277 nm and corresponds to the group chromophore carbonyl (C = O), the dominant electronic transition is a  $\pi \rightarrow \pi^*$  type (Fig 3.32).

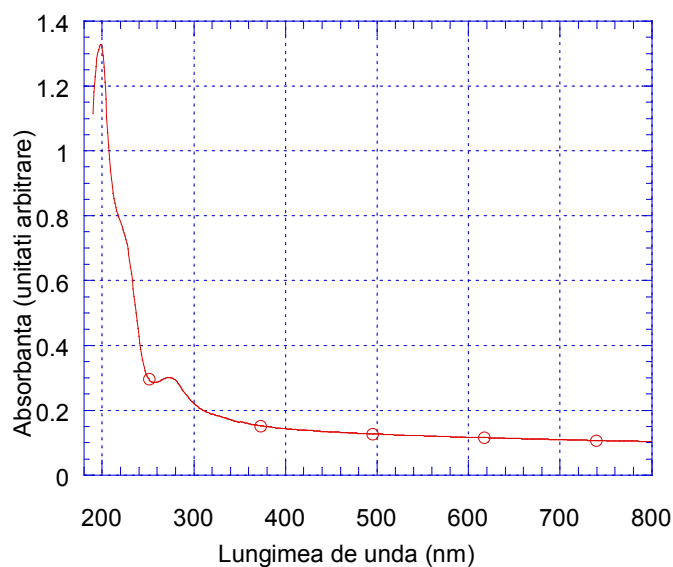


Fig. 3.3.2. UV-Vis absorption spectra for pure PVA.

After doping, it was observed that, if the concentration of TiO<sub>2</sub> increases, the absorption maximum occurs at the same wavelength (277 nm), but the magnitude continuously increased, being substantially higher than that of the undoped membrane, (Figure 3.3.3).

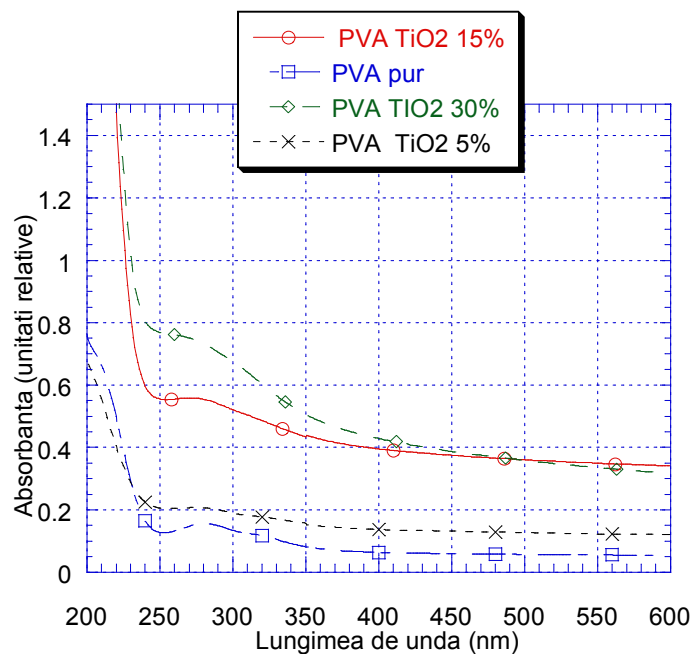


Figure 3.3.3. UV -VIS absorption spectra for pure and TiO<sub>2</sub>doped PVA membranes.

After gamma irradiation, it was observed a pronounced increase of absorption maximum at 277 nm and the monotonous increase of the absorbance between 500 and 300 nm (Figure 3.34). Increasing the absorption coefficient at 277 nm in the UV indicates that gamma irradiation increases the abundance molecular species with properties of chromophores. At this wavelength, the carbonyl group strongly absorbs UV. Sharp increase in the percentage of carbonyl groups after irradiation can be explained by cleavage of the hydroxyl and carbonyl double bond formation after polymer chain breakage.

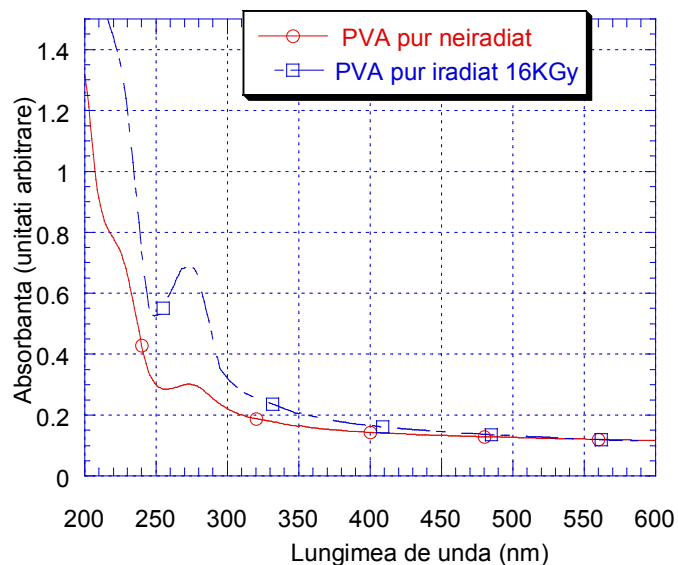


Figure 3.3.4 UV-Vis absorption spectra for pure and gamma irradiated with 16 KGy PVA membranes.

### 3.3.2. Raman investigations

Pure PVA shows well-defined bands in the  $1200 - 1600 \text{ cm}^{-1}$ . The most intense bands are assigned as follows:  $1287 \text{ cm}^{-1}$  - CH rocking (wagging),  $1362 \text{ cm}^{-1}$  - CH bending (bending) and OH - bending (bending),  $1415 \text{ cm}^{-1}$  -  $\text{CH}_2$  bending (bending) (Fig. 3.36).

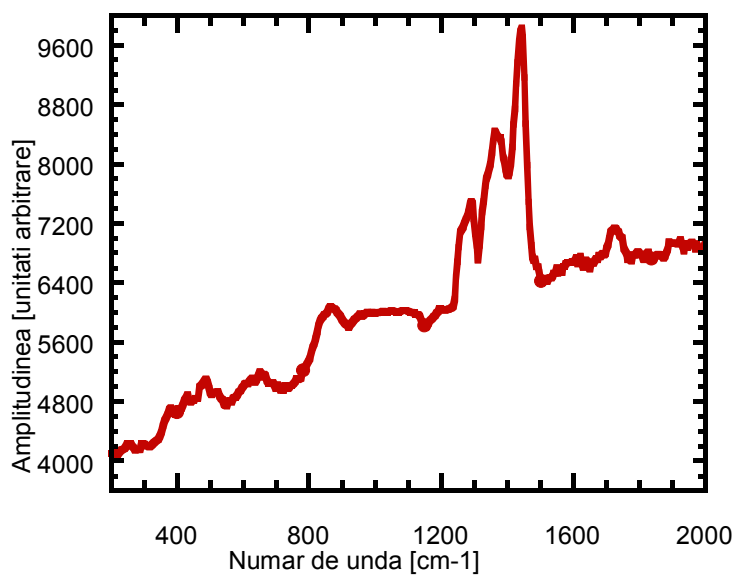


Figure 3.3.6 Raman spectra of pure PVA membrane.

After doping with  $\text{TiO}_2$  in the frequency spectrum of pure PVA additional bands appear due to dopant. These additional bands due PVA doping  $\text{TiO}_2$  appear at  $400 \text{ cm}^{-1}$ ,  $514 \text{ cm}^{-1}$  and  $638 \text{ cm}^{-1}$ , the amplitude increased with increasing the concentration of  $\text{TiO}_2$  (Fig 3.3.7).

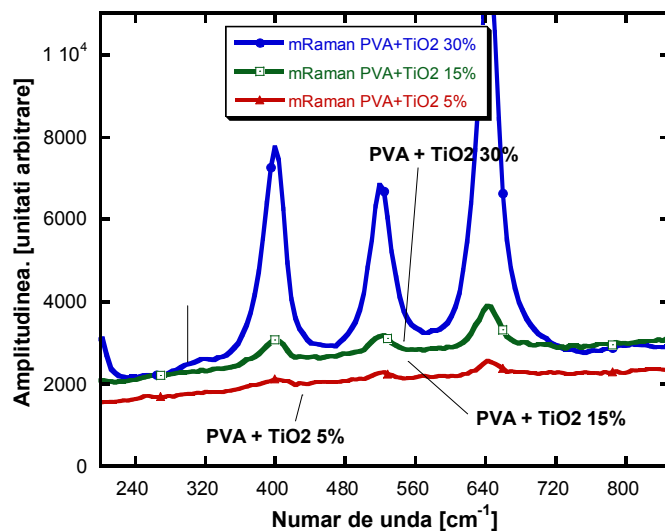


Figure 3.3.7 Raman spectra of PVA membranes doped with 5.15 and 30% TiO<sub>2</sub>.

After intense gamma irradiation with a dose of 16KGy accumulation is observed strong blurring characteristic vibrational bands of pure PVA, (Figure 3.3.9), due to changes caused by radiation due to cleavage of bonds.

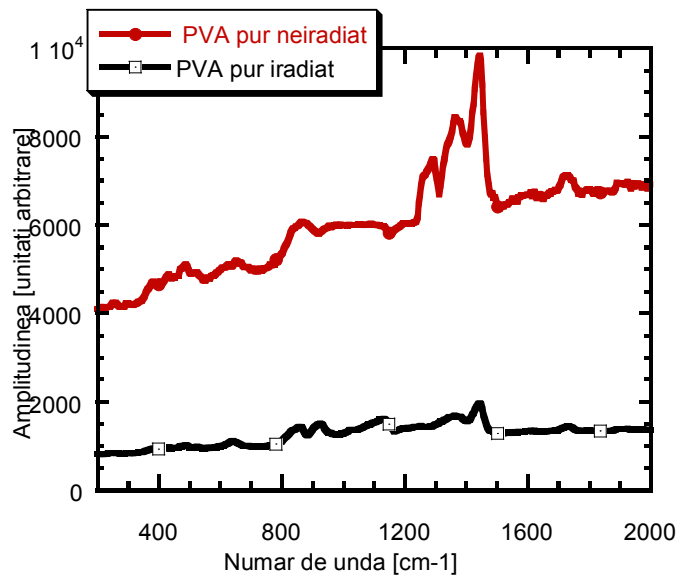


Figure 3.39 Raman spectra of pure PVA membrane gamma irradiated and irradiated with 16 KGy.

### 3.3.3. Investigation by EPR

The existence of paramagnetic species, such as free radicals or unpaired electrons, before and especially after the gamma radiation, can be accurately highlighted appealing to ESR spectroscopy. After gamma irradiation of macromolecules cleavages occur with the formation of electrons and free radicals. This phenomenon is evidenced by EPR spectra of pure PVA membrane (Fig 3.42). If PVA doped  $\text{TiO}_2$  dopant is observed that induces a protective effect of gamma irradiation from polymer matrix. Thus it is found that at a given radiation dose is greater than the amplitude of the EPR signal from the sample with low concentration of  $\text{TiO}_2$ . Amplitude decreases monotonically with increasing concentration of  $\text{TiO}_2$ . (Fig 3.43).

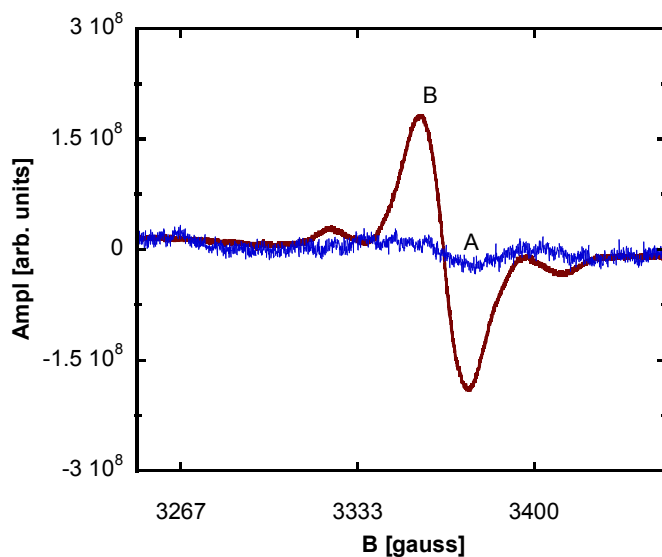


Fig. 3.42. The EPR spectrum of pure PVA irradiated (curve A) and after gamma irradiation with a dose of 16 kGy (curve B)

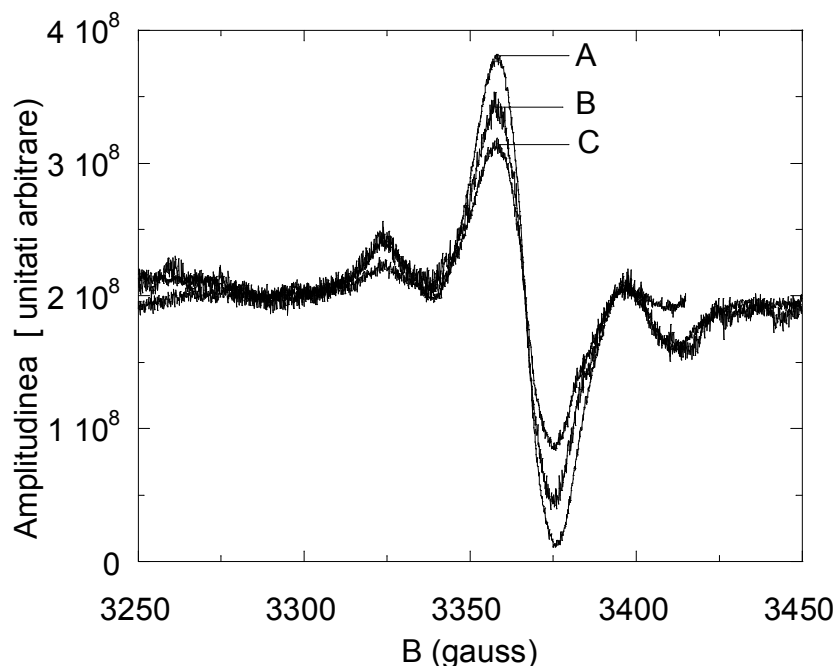


Figure 3.43. EPR spectrum of the PVA membrane 16 KGy. A gamma irradiated TiO<sub>2</sub>. A 10% TiO<sub>2</sub>, B TiO<sub>2</sub> -20 % C- 30 % TiO<sub>2</sub>

### 3.3.4. Investigations by X-ray diffraction

The XRD diffractograms for pure PVA before irradiation shows a broad signal between 10 ° and 22 °, with three levels (Fig.3.46.). The crystalline phase of the PVA has a maximum diffraction at  $2\theta = 19^\circ$  which corresponds to a mixture and parallel planes such as (101) and (10-1) [13]. Increasing this maximum is determined by the crystalline phase at the expense of increasing the amorphous phase [16, 21]. This maximum can be observed in the diffractogram recorded for pure PVA at  $2\theta = 19.6^\circ$ , which indicates a significant amount of crystalline phase. The other two peaks can be observed in the  $2\theta = 13.5^\circ$  and  $16.3^\circ$ . They are caused by diffraction of the planes (100) and (00-1). After irradiation it decreases the amplitude peaks  $2\theta = 13.5^\circ$  and at  $2\theta = 19.6^\circ$ , a phenomenon associated with decreased concentration of crystalline phase due to local destruction order after splitting macromolecules. Doping TiO<sub>2</sub> crystallinity leads to increased progressively with increasing dose dopant compound, (Fig 3.48).

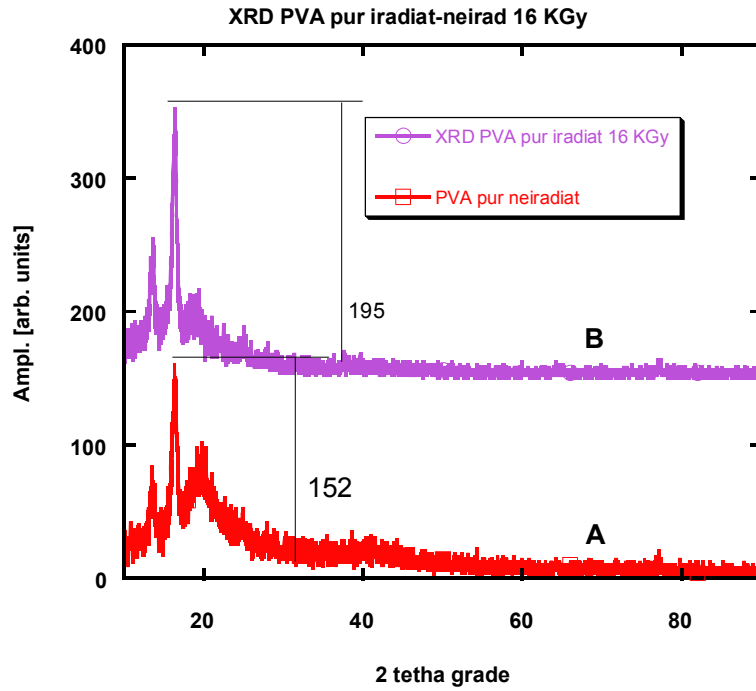


Fig. 3.46 The diffractogram of pure PVA before irradiation (curve A) or gamma irradiated at a dose of 16 KGy (curve B).

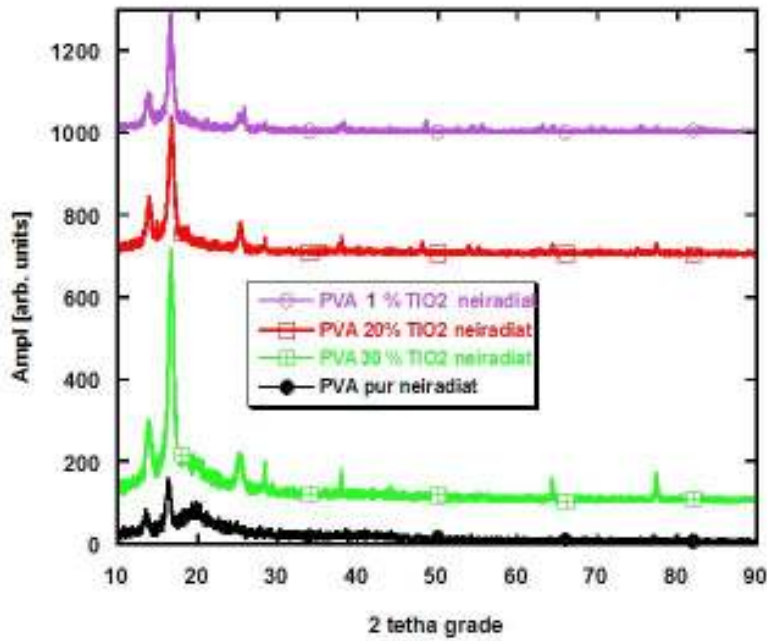


Fig. 3.48 . Pure PVA or PVA diffraction doped with 1, 20, 30 % TiO<sub>2</sub> irradiated.

### 3.3.5. DSC investigations of PVA membranes doped with TiO<sub>2</sub>

It finds widening the temperature range between melting occurs as lower percentage of impurities in TiO<sub>2</sub>. Thus, if the sample with 30 % TiO<sub>2</sub> melting takes place at 500 ° C ( Fig. 3.52 ) for the 1 % TiO<sub>2</sub> this range is between 400 ° and 560 ° C ( Fig 3.54 ) melting a wider range of temperatures is typical of amorphous substances or a low degree of crystallinity the total crystalline melting at a constant temperature. Increasing doping TiO<sub>2</sub> crystalline phase has the effect of increasing the expense of PVA amorphous phase.

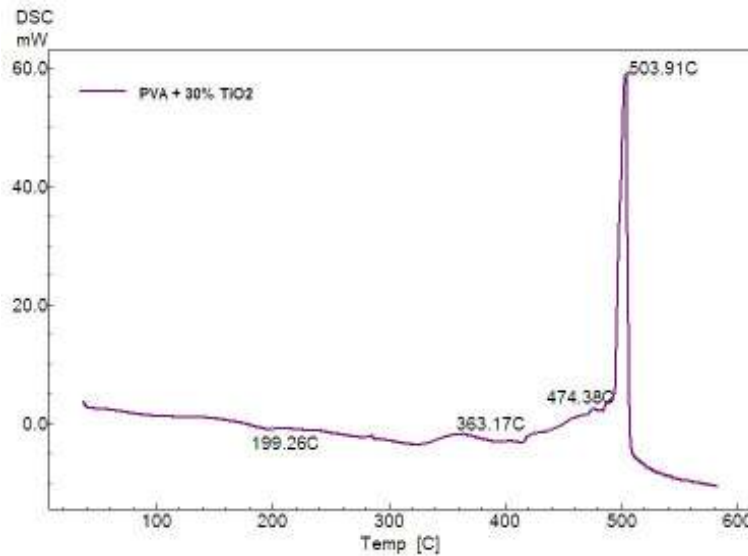


Figure 3.52. The thermogram of PVA sample doped with 30% TiO<sub>2</sub>.

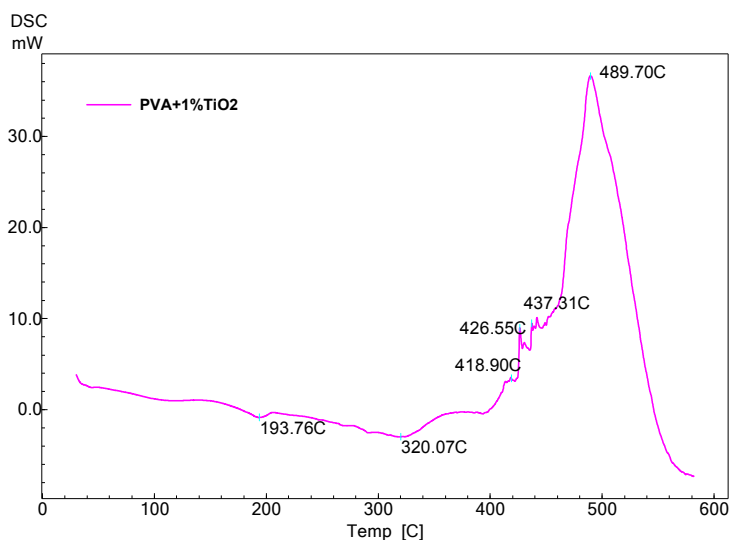


Figure 3.54. The sample thermogram of PVA doped with 1% TiO<sub>2</sub>

### 3.4. Spectroscopic Investigation of pure and carbon doped PVA membranes

#### 3.4.1. IR investigations of pure PVA membranes and carbon doped

Some of the most intense bands of the IR spectrum of pure PVA are assigned as follows:  $798\text{ cm}^{-1}$  C-C stretching,  $1161\text{ cm}^{-1}$  CC stretching and OH bending, CO stretching  $1241\text{ cm}^{-1}$ ,  $1440\text{ cm}^{-1}$  - CH OH bending and bending,  $1704\text{ cm}^{-1}$  C = O stretching,  $2912\text{ cm}^{-1}$ -CH stretching (Fig.3.55.)

Following low carbon doping we find keeping unmodified PVA characteristic vibrational bands and the appearance of additional bands at  $1022\text{ cm}^{-1}$  due to carbon. (Fig 3.56)

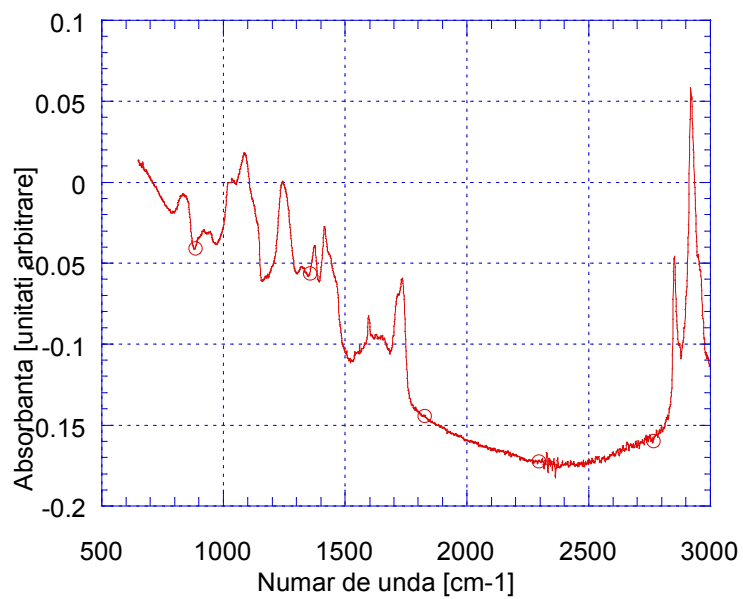


Fig3.55. The IR spectra of pure PVA membrane.

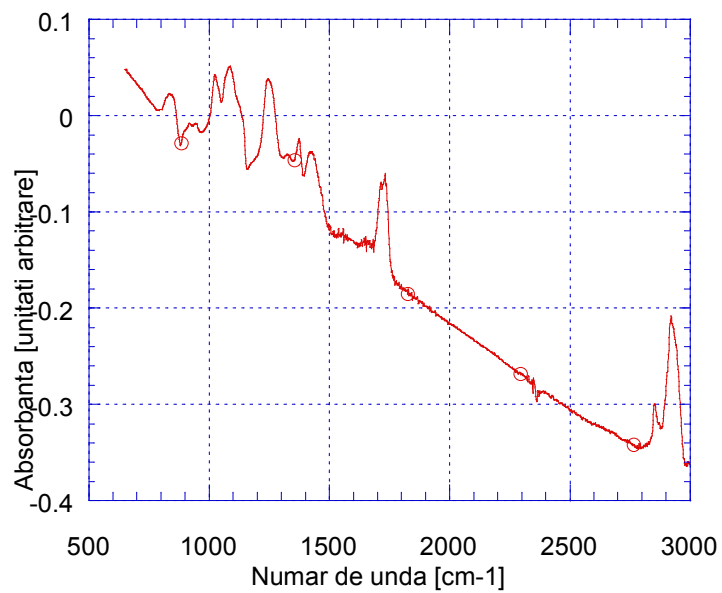


Figure 3.56. The IR spectrum of the PVA membrane doped with 1% carbon

### 3.4.2. UV-VIS measurements

In the case of pure PVA have an absorption maximum at 277 nm with an absorption band width of approx. 20 nm (Fig3.59 and Fig. 3.32.), The mechanism of absorption is described.

Absorption spectrum was recorded in UV-VIS for PVA-Carbon compound for different percentages of doping against specific spectrum of pure PVA. For PVA doped Carbon storage is distinguished from the maximum of 277 nm absorption characteristic of pure PVA bandwidth to 20 nm to the absorbance curves translate proportionately higher carbon content increases in the mixture, (Fig3.59).

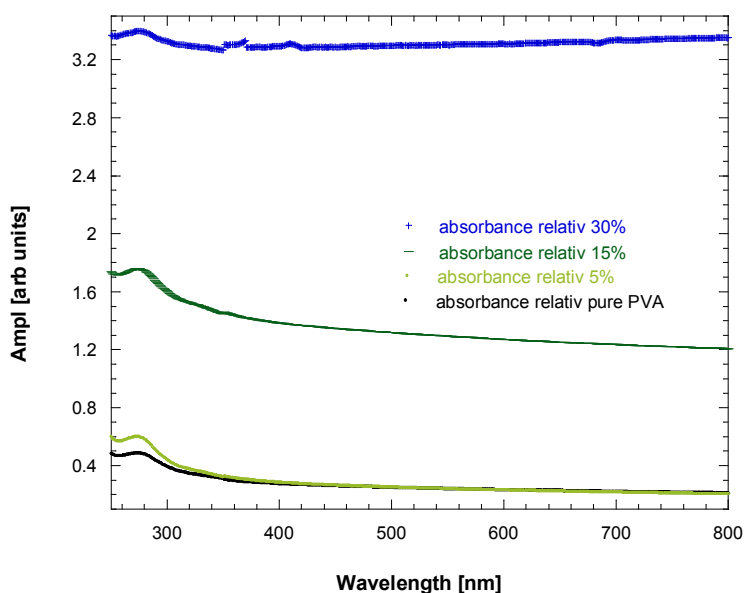


Figure 3.59. The UV -VIS absorption spectra of pure and doped PVA membranes of 5.15 and 30 % carbon.

### 3.4.3. Raman investigation

The major bands observed in the spectrum of pure PVA is located at  $1710\text{ cm}^{-1}$ ,  $1440\text{ cm}^{-1}$ , corresponding to the bending vibrations of CH and OH group,  $1232\text{ cm}^{-1}$  corresponds to the swing CH  $1145\text{ cm}^{-1}$  corresponding to CO and bending CC,  $918\text{ cm}^{-1}$  and  $856\text{ cm}^{-1}$  corresponding to the DC torque, ( Fig.3.62 ).

After doping with carbon is found that the presence of dopant in the vicinity of polymer segments can induce a small change of the vibrational modes of chemical bonds of the monomer. In order to observe possible changes we recorded spectra for pure PVA and then spectrum membranes doped (Fig.3.62). Doped sample peaks appear belonging to the following wave numbers:  $1710\text{ cm}^{-1}$ ,  $1598\text{ cm}^{-1}$ ,  $1440\text{ cm}^{-1}$ ,  $1349\text{ cm}^{-1}$ ,  $1232\text{ cm}^{-1}$ ,  $1145\text{ cm}^{-1}$ ,  $918\text{ cm}^{-1}$  and  $856\text{ cm}^{-1}$ . Raman spectra of the doped membranes were recorded for different concentrations of carbon of 1 % to 50 %. Such a spectrum contains specific bands vibrations of pure PVA values located at 1710, 1440, 1232, 1145, 918 and  $856\text{ cm}^{-1}$ . In addition, two intense bands were observed at  $1349\text{ cm}^{-1}$  and  $1598\text{ cm}^{-1}$ . Their magnitude increases significantly with increasing carbon concentration, while other bands remain almost constant amplitude (Fig.3.62). Knowing that the amplitude of vibration bands increases with the number of chemical bonds involved in these vibrations, we conclude that these links belong carbon dopant. On the other hand, the position of the specific bands vibrations of PVA does not change with increasing dopant concentration. Raman spectra of doped membranes contain characteristic bands of pure PVA plus corresponding amorphous carbon bands. Consequently, the doped sample spectrum appears as a simple superposition of the spectra. Each component of this combination keeps its own identity, so intermolecular bonds are weak physical links. From this observation we conclude that there are new chemical bonds between the dopant and the polymer matrix.

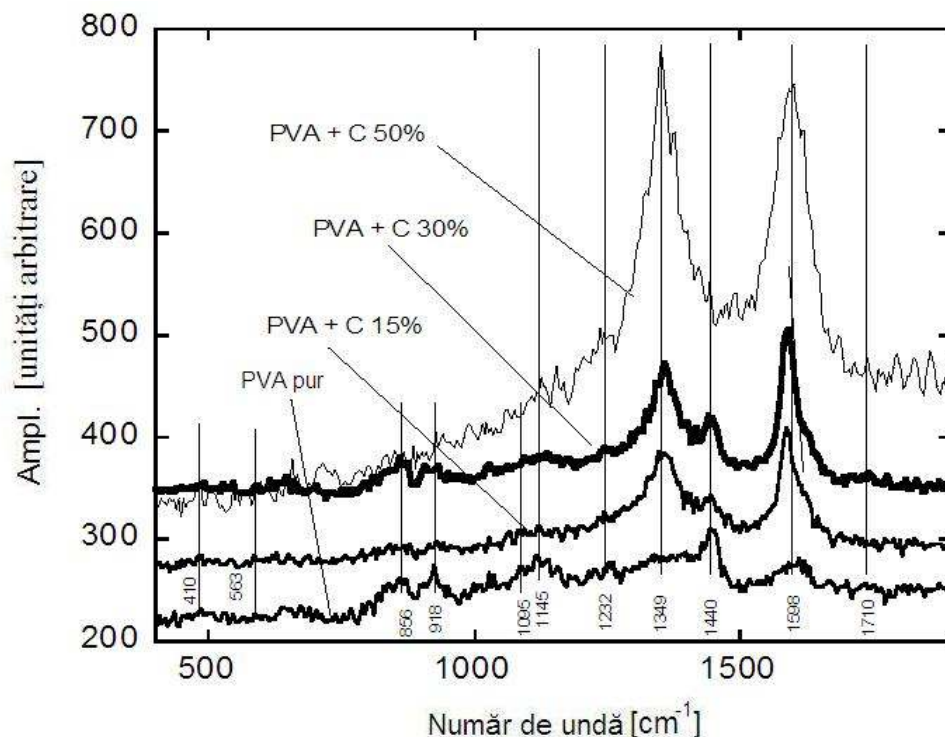


Fig.3.62 . The Raman spectra of pure and doped PVA membranes with 15, 30 and 50 % carbon.

### 3.4.4 . XRD investigations

XRD patterns recorded for pure PVA samples were previously presented (Fig.3.46). We reported the appearance of a broad diffraction peaks centred 9 angle,  $6^\circ$  (Fig.3.64). This maximum is caused by the existence of a small percentage of the ordered phase in the polymer matrix constitution.

X-ray diffraction of PVA membranes doped with carbon containing specific peaks of pure PVA at  $2\theta = 19.6^\circ$  and another peak at  $2\theta = 25^\circ$  characteristic of carbon . The amplitude of this maximum increases with increasing carbon concentration (Fig. 3.64). The fact that increasing carbon concentration causing increased specific diffraction peaks indicate increasing PVA crystalline phase of the compound due to the presence of carbon. By creating new connections causing reduced intermolecular carbon molecular

dynamics and network hardening effect of having the appearance of new planes of reflection and ordered phases in the compound.

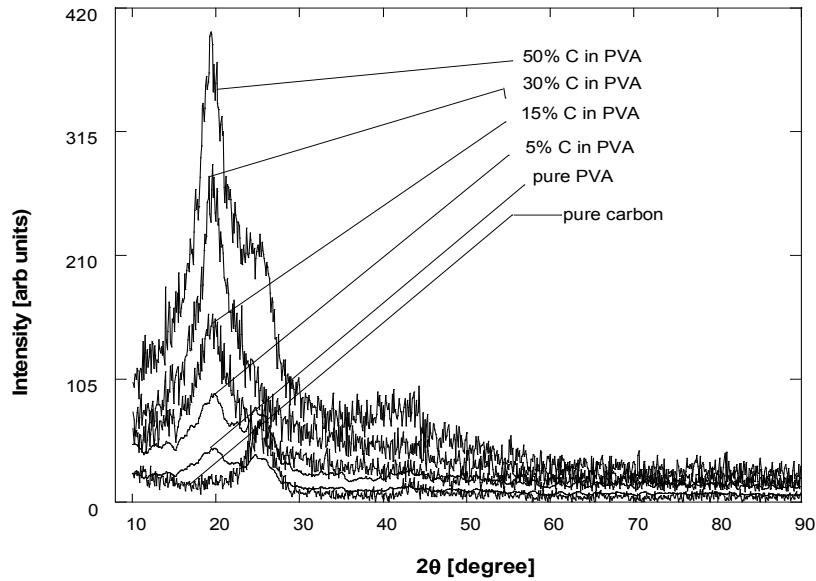


Figure 3.64. The diffractogram of pure carbon, pure PVA, and PVA doped with, respectively, 5, 15, 30 and 50% carbon.

After gamma irradiation at a dose of approx. 9 KGy, the amplitude decrease is observed diffraction peaks corresponding to pure PVA, (Fig 3.65). This behaviour can be attributed to changes in the local order of the polymer chains due to possible breakage due to irradiation. After shortening these chains become more mobile, local order decreases and the crystalline phase of the polymer diminishes in favour of amorphous phase. However comparison of the XRD spectra before and after irradiation doped membranes show moderate changes, indicating generally good stability of the system (Figure 3.65). Also, these findings are in agreement with Raman observations.

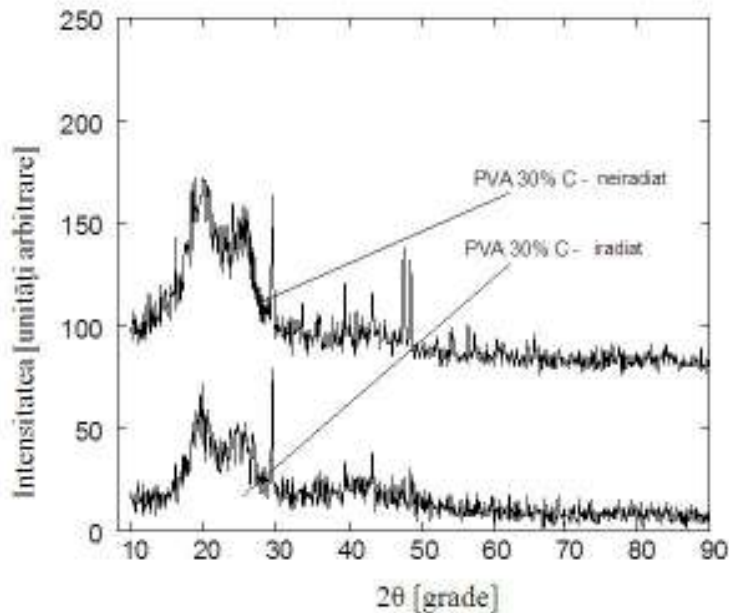


Figure 3.65. The diffractogram for PVA samples doped with 30% carbon gamma - irradiated and irradiated

### 3.4.5 . ESR Investigation of PVA membranes doped with carbon

PVA membranes doped with carbon from carbon shows paramagnetic properties included. They absorb the microwave energy and show a field of resonance signal which is higher if the concentration of carbon increases. Thus EPR signal amplitude for 30% carbon concentration is greater than the amplitude corresponding to 15% carbon concentration in PVA (Fig 3.67).

After gamma irradiation is observed appreciably greater resonance signal which means increasing the number of resulting unpaired electrons breaking of covalent links. Increasing the amplitude of resonant signals after irradiation is not proportional to the increase of carbon concentration in samples and do not respect the relationship between the amplitude of the resonance signals corresponding to different concentrations before irradiation.

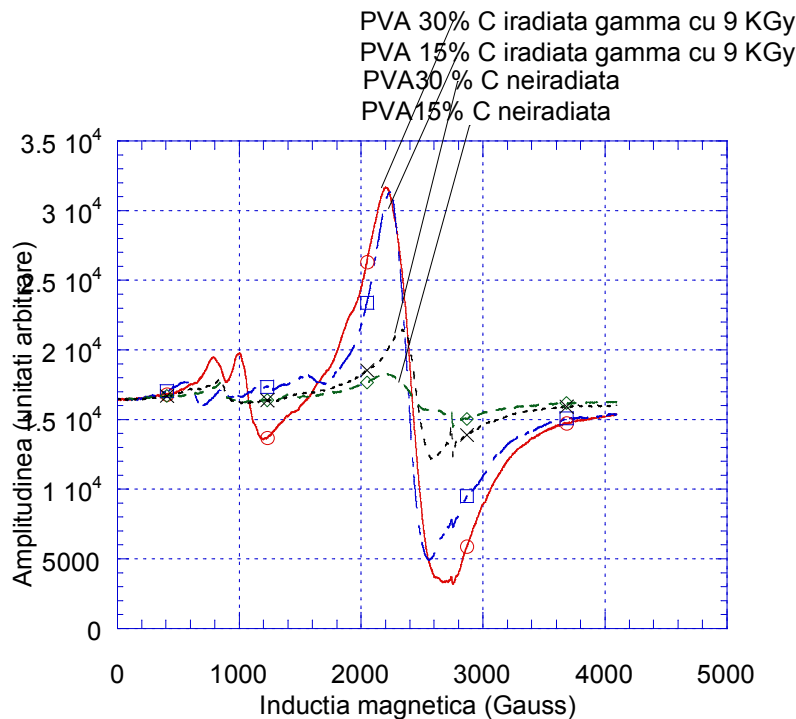


Figure 3.67. The ESR spectra of PVA -C membranes doped with 15 and 30% , non-irradiated and irradiated by 9 KGy.

## Chapter 4. Polymer electrodes fuel cells

The PVA membranes doped with  $\text{TiO}_2$  and carbon, which were electrical and spectroscopic investigated, were used for assembling and testing electric fuel cells. Low resistivity PVA was presented after contamination with carbon and the high chemical stability of the compound made possible to use it as polymer electrodes for these cells. The high resistivity offered by  $\text{TiO}_2$  doping made possible to use it as solid electrolyte compound with directed proton transfer. Spectroscopic investigations have shown the effect of gamma irradiation on destructive the polymer matrix followed by molecular rearrangements to yield the same effect by treating with hot polymer complex chemical solutions to fulfil certain requirements imposed by the use of the solid electrolyte cells. Therefore, the experiments were also used with favourable results, irradiated PVA membranes doped with  $\text{TiO}_2$ .

### 4.1 Use of PVA membranes doped $\text{TiO}_2$ and carbon in fuel cells

PVA membranes doped TiO<sub>2</sub> shows in fluid environments super acidic membrane properties because they can provide easily under the influence of an electrochemical potential gradient transfer of protons (H<sup>+</sup>) between compartments that separate them. Because of this quality, it was attempted to use methanol fuel cells (DMFC) with the role of separator positive charges directed transfer between reactants. Attempts to introduce these membranes in fuel cell construction is an economically attractive solution being cheaper than Nafion membranes that are already established and being the first type of membranes with this destination. A few authors have reported positive results in their experimental research fuel cell assemblies having as separator ionic PVA doped TiO<sub>2</sub> chemically treated to improve the structure (cross-linking) and as electrodes paper that has been deposited carbon layer combined with catalysts. Starting from the premise of increasing yield by increasing surface and elongated proton exchange reaction inside the catalytic layer I tried with favourable results using polymer electrode having as strong support throughout PVA doped with carbon in order to ensure electronic conductivity. I also experienced replacement treatment chemically complex membrane separators (PVA doped TiO<sub>2</sub>) by irradiating them with high doses of gamma radiation whose effect has proven beneficial for this application. Chemically untreated membranes permeability shows inadequate (too high) for working solution in methanol and liquid retention adverse effect on performance. After treatment macromolecules undergo reorientation processes, parallelism certain areas which is predominant macromolecular initial state being disorganized by the appearance of numerous crosses and random orientation of macromolecular chains. This structural change is achieved by heat treatment of the membrane in concentrated solutions of GA (glutaraldehyde) and HCl [5]. GA is all too toxic and expensive.

We found that high-dose gamma irradiation effects similar structural changes of macromolecules followed by cleavage of the membrane rearrangements affording their properties close to those of membranes undergo chemical treatment.

#### **4.2 Experimentation PVA polymer membranes in DMFC construction**

I experienced the realization of some elementary fuel cells using as solid membranes of PVA + 30% TiO<sub>2</sub>, chemically treated with GA and HCl, PVA 50% carbon, as anode, with a catalytic load of 10 mg/cm<sup>2</sup> Ni and Zn particles, in equal amounts, and 50% PVA as carbon cathode, with a catalytic load of 6 mg/cm<sup>2</sup> MnO<sub>2</sub>. I also used other combinations of anodic catalysts consisting of Pt-Ni, Pt-Sn, Pt-Zn (ultrafine platinum nanoparticles of platinum hexachloride) and also Ni-Sn. (Table 4.1.).

After hot pressing, I have obtained a membrane with a thickness of 5 mm, while the anode and cathode were remaining porous enough. Active area of the cell is 2 cm<sup>2</sup> being determined by the circular area of the two jaws of the press. The fuel used was 65% methanol in water (10 M) and the oxidant was the oxygen from the air. The measured electrical parameters were U = 0.220 V and I = 0.022 A at a load of 10 Ω (100 mA scale analogue ampermeter Ri = 1.6 Ω), which corresponds to a power of 2.42 mW for an area of 1 cm<sup>2</sup> (Table 4.1.).

When using the gamma irradiated membrane, at a dose of 16 KGy, after a relaxation period of 30 days, instead of chemically treated membrane, the electrical parameters were measured in the same conditions: U = 0.220 V and I = 0.009 A, corresponding to a power of 1.98 mW, which indicates a power loss of approx. 20% compared to the previous situation (Fig.4.3.).

In the case of PVA + TiO<sub>2</sub> membrane, chemically untreated and irradiated, the power loss was about 65% and the time stability of the cell parameters was affected (after an hour of experiment, it was observed a noticeable decrease in performance). We assume that irradiation may be useful in obtaining structural changes in the polymeric matrix, which are necessary in some applications.

Although the performances of these cells were lower than Nafion catalysts, using noble metal catalysts, and whose power reached approx. 17 mW/cm<sup>2</sup>, the low price and the availability of components used is an advantage that justifies their study. When using noble metal catalysts (Pt, Ru), the performance of the cells with an ion separator of PVA + TiO<sub>2</sub> are comparable to those of Nafion (Table 4.1).

Table 4.1. Some basic electrical performance of fuel cells with methanol and air for 1 cm<sup>2</sup> active area, in the environmental temperature. The separation membrane is of PVA

doped with TiO<sub>2</sub> and the electrodes are made of PVA with carbon, excepting the mentioned situations.

PVA+TiO <sub>2</sub> membrane, chemically untreated and unirradiated	U =0,220V 10Ω	I =4 mA	P=0.88 mW	With non-noble catalysts of Ni-Zn
The gamma irradiated membrane, 16 KGy	U =0.220V 10Ω	I =9 mA	P=1.98 mW	With non-noble catalysts of Ni-Zn
Chemically treated membrane, electrodes deposited on the paper			P=1.5 mW	With non-noble catalysts (literature data)
Chemically treated membrane with GA, HCl and acetone	U =0,220V 10Ω	I =12 mA	P=2.42 mW	With non-noble catalysts of Ni-Zn
The gamma irradiated membrane, 16 KGy	U =0.340V 10Ω	I =30 mA	P=10.2 mW	Pt and Ni catalyst
Chemically treated membrane with GA, HCl and acetone	U =0.340V 10Ω	I =38 mA	P=12.92 mW	Pt and Ni catalyst
Nafion membrane	U=0.355V	I=42 mA	P=14.91 mW	Pt and Ni

	10Ω			catalyst
Nafion membrane			P=17.1mW	Pt-Ru catalyst (literature data)

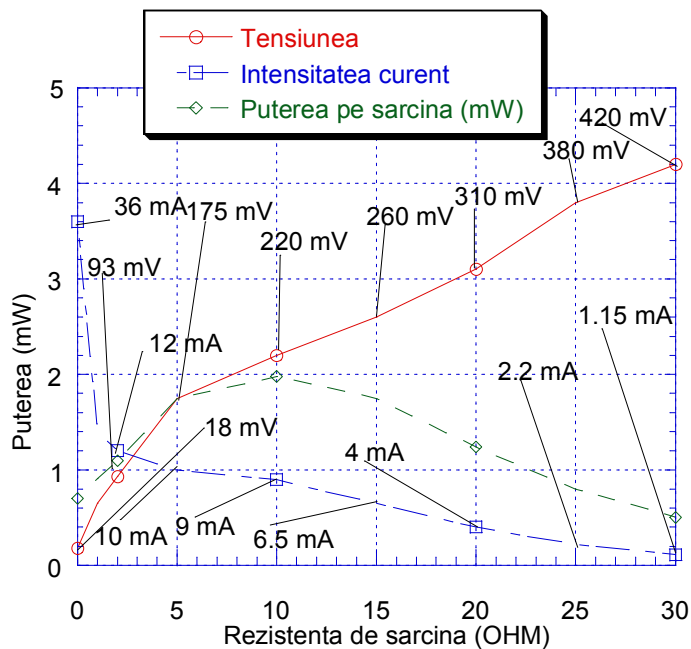


Fig.4.3. The dependence of voltage, current and power of the external resistance for the cell membrane PVA - TiO<sub>2</sub> 16 KGy gamma irradiated with PVA - Carbon electrodes and Ni- Zn anode catalysts, respectively cathodes, of MnO<sub>2</sub>, for the active area of 1 cm<sup>2</sup>.

## CHAPTER 5 Spectroscopic Investigation of PAA membranes

This chapter presents the results of spectroscopic investigations of carbon doped PAA membranes that TiO<sub>2</sub>.care shows multiple practical applications, especially in pharmacology.

## 5.1 Spectroscopic Investigation of carbon-doped PAA membranes

### 5.1.1 UV-VIS investigations

Pure membrane shows good transparency in the range 250-800 nm, with an absorption maximum at 207 nm (Figure 5. 1).

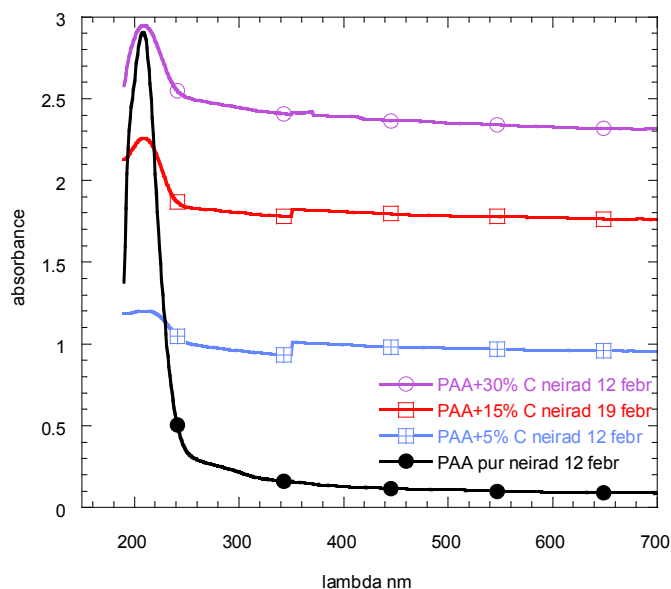


Figure 5.1 Absorption spectra for pure PAA membrane and 5.15% and 30% carbon doped.

After adding carbon, the absorption throughout the UV-VIS increases significantly. For example, the carbon concentration of 15% is absorbed in 70% and 30% is 135% higher than the absorbance of 5%. However, the characteristic absorption peak of PAA can be seen again in the spectrum at the same wavelength as the pure PAA membrane (Figure 5. 1). Membranes doped spectra appear as a superposition of spectra of pure carbon and pure polymer. The composite material combines the features of both components, each component keeping unaltered its optical properties. From these observations it appears that the addition of carbon does not alter the chemical structure of the polymer.

### 5.1.2. XRD investigations

From the diffractogram of pure PAA membrane can be observed central dispersion diffraction angle. The diffractogram is characterized by an intense and broad signal centred angle  $2\theta = 17.2^\circ$  and shoulder more intensely  $2\theta = 35^\circ$  in agreement with other works (Fig.5.2).

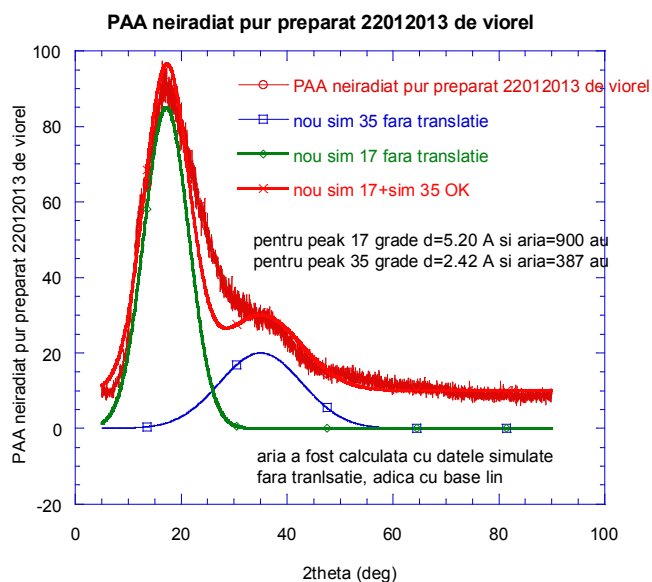


Fig 5.2. The PAA sample diffractogram and the spectrum deconvolution.

This diffractogram is the result of the superposition of two diffraction peaks which can be clearly seen only by simulation and deconvolution of the spectrum. Each peak was approximated by Gaussian function centred on the diffraction angle, considering the amplitude and width as variables. These parameters were adjusted until a good agreement was obtained between the experimental and calculated (Fig.5. 2).

After irradiation, no significant changes were observed. Maxima occur at the same angles of diffraction their width remains unchanged but the amplitude decreases slightly, and accordingly, the area under the peak decreases accordingly, (Fig.5.4.). The amplitude of the peak simulated is 69 and 17 and the areas under the peak areas were 731 and 331 have. This means that after irradiation no change of interplanar distances or quantities ordered phases but only a slight modification of the total concentration of

crystalline phase in the sample. This decrease is caused by the breakdown phase ordered chains induced by irradiation followed by increased local dynamics and their repositioning.

XRD spectrum was recorded for PAA doped carbon observing changes ordered structure of the polymer after doping. To this end we investigated the pure dopant, (graphite) and then doped samples. In experiments pure graphite diffraction diagram contains two important maximum  $2\theta = 25.2^\circ$  and  $2\theta = 43^\circ$  that occur with different intensities and a weak maximum at  $2\theta = 55^\circ$ . (Fig.5.5.).

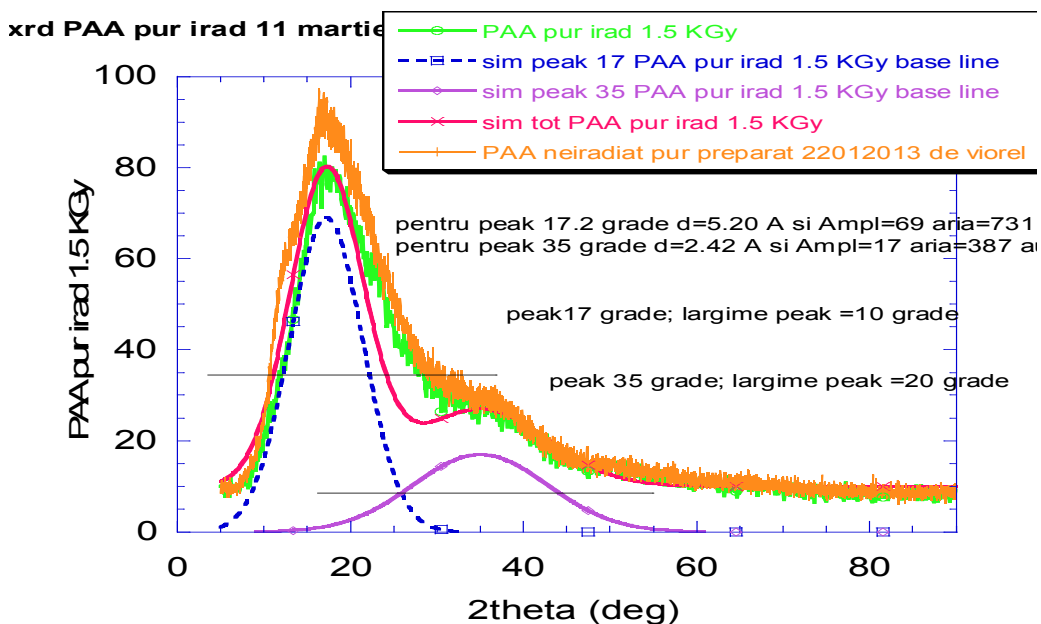


Fig.5.4. The diffractogram for pure unirradiated PAA, gamma irradiated (1.5 KGy) PAA and the deconvolution of spectra.

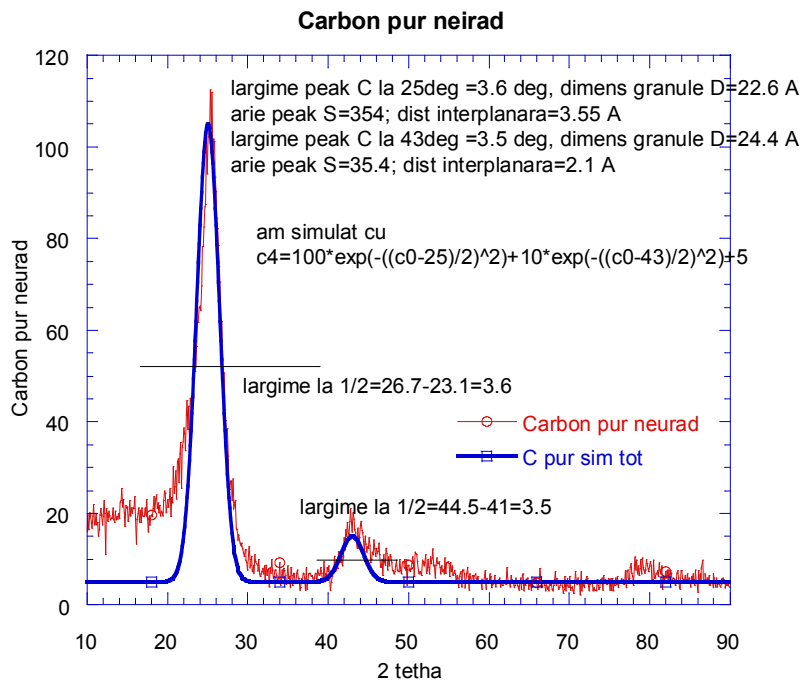


Fig. 5.5. The diffractogram of irradiated pure carbon.

Doped samples were subsequently investigated. The diffractogram of the composite material appears as a superposition of the spectra of the two components. (Fig.5.6 and Fig.5.7). Doped samples contain characteristics of PAA's high and graphite's no significant change in the diffraction angles, but with different amplitudes depending on the concentration of graphite. Thus, a low concentration of carbon, namely 5% graphite specific peaks are barely due to overlapping with peaks which are wide and high. When the concentration of carbon increases, the peaks generated by graphite become more apparent and appear clearer diffraction pattern (Fig.5.6.). However, whatever the dopant concentration, the parameters of the peaks, amplitude, width and area may be measured quantitatively diffraction only after simulation. An example is shown in Figure 5.8. the concentration of 30% carbon. At this concentration the first peak of PAA changes from  $2\theta = 17.2^\circ$  at  $2\theta = 18.2^\circ$  and line width at medium height increases from  $9^\circ$  to  $10^\circ$ . This is equivalent to a change in the interplanar distance of  $4.86 \text{ \AA}$  and  $5.15 \text{ \AA}$  to change the size ordered phase from  $8.9 \text{ \AA}$  to  $8.06 \text{ \AA}$ . Ordered phases of the polymer becomes more compact in the presence of graphite. These results suggest

reluctance by graphite polymer chain, thereby forcing the polymer to adopt a more compact structure. The parameters are compared with those of the irradiated sample to observe the effect of radiation. After irradiation, the concentration of 30% carbon diffraction peaks of PAA's appearing at the angles  $2\theta = 18^\circ$  and  $2\theta = 35^\circ$  amplitude  $A = 68$  and  $A = 21$ , width lines at medium height being  $\beta = 10^\circ$  and  $19^\circ$  and the corresponding areas were respectively  $S = 720$   $S = 398$  have. (Fig. 5.8). Report from the areas under the peaks of PAA's and graphite from the site before irradiation and after irradiation is 3.29 is 3.69. The area under the peak is proportional to the concentration of the ordered phase, it follows that there is a decrease in the degree of order in the polymer after irradiation. This behavior can be explained if we assume that irradiation produces an effect of breaking the polymer chains, followed by increasing their growth and consequently, a decrease in local order.

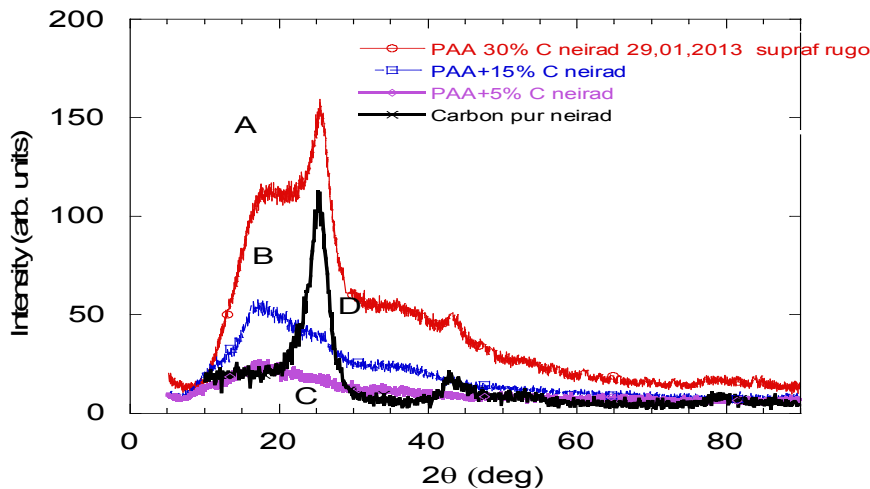


Fig.5.6. The pure carbon diffractogram (B), 5% carbon PAA (C), 15% carbon PAA (D) and 30% carbon PAA (A).

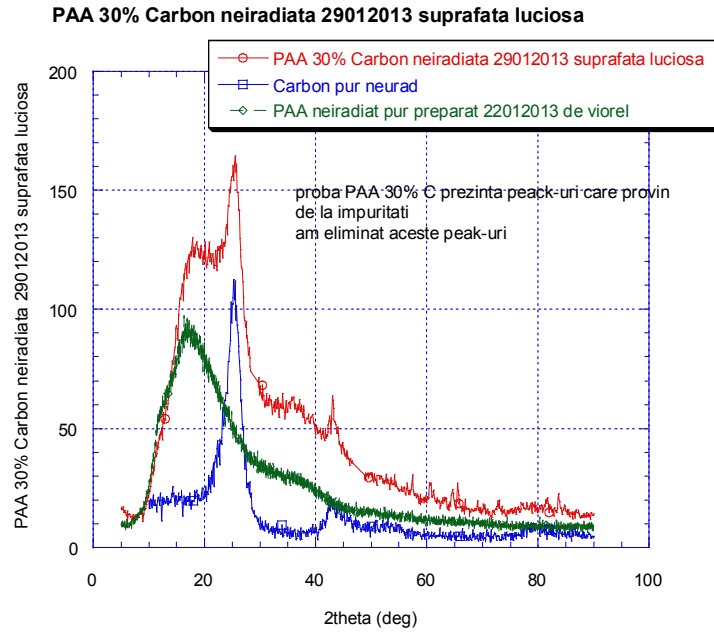


Fig.5.7. The pure PAA diffractogram, 30% Carbon doped PAA and pure Carbon.

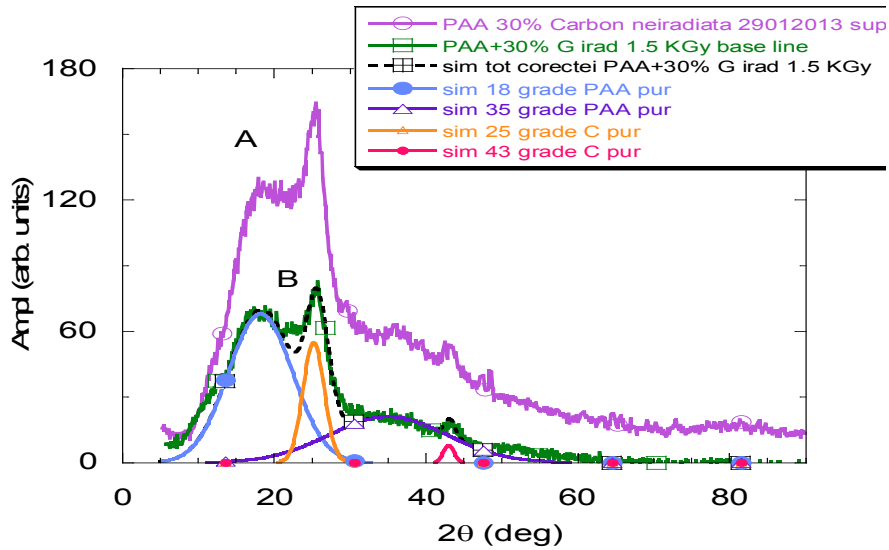


Fig.5.8. The PAA sample diffractogram. 30% carbon unirradiated (A) and irradiated with 1.5 KGy (B) and the simulation of each maximum, respectively, of full spectrum, for the irradiated sample.

### 5.1.3. ESR Investigation of PAA-Carbon membranes

Simple monomer polymers such as PVA (or PAA) containing only atoms as C, H, O, usually do not give any ESR signal, all valence electrons were included in saturated bonds. This is illustrated by the ESR spectrum of the PAA membrane just before irradiation (Fig.5.9. Curve A). Basically, the sample does not give any ESR signal.

After the gamma irradiation dose of 1.5 kGy, due to the macromolecules divisions, the paramagnetic species occur, highlighted by the weak RES signal. (Fig.5.9. Curve B).

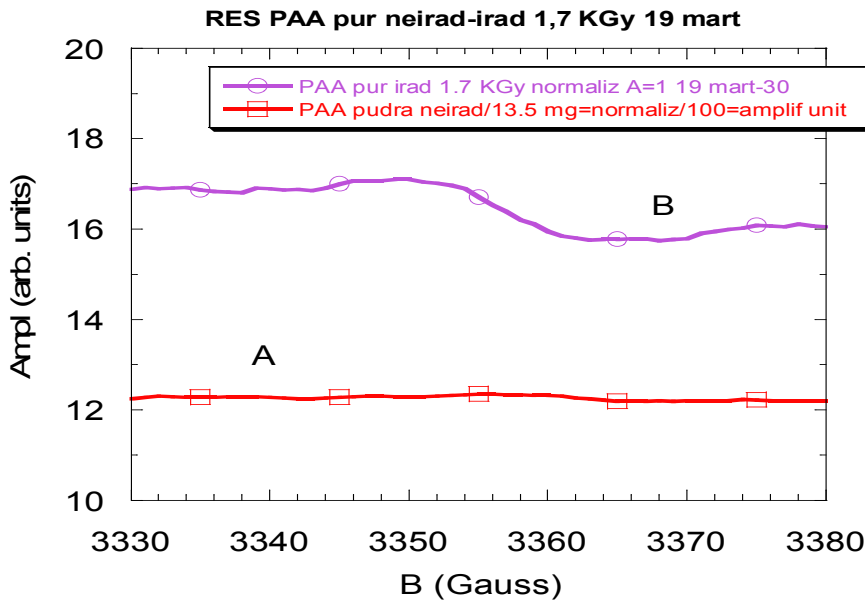


Fig. 5.9. The ESR spectra of unirradiated pure PAA membrane (A) and irradiated with 1.5 KGy (B).

The introduction of small amounts of graphite in the polymer matrix causes a strong and sharp signal without hyperfine structure. For all concentrations, the signal is centred at 3,357 Gs, equivalent to a gyromagnetic factor  $g = 2.002$ .

This value of the gyromagnetic factor corresponds to the existence of paramagnetic electrons. The amplitude gradually increases with the concentration of graphite (Fig. 5.11.).

From this behaviour and knowing that the polymer did not give any signal before irradiation, we concluded that the RES signal is provided only for samples doped with

graphite. This signal is exclusively determined by the unpaired electrons belonging to graphite.

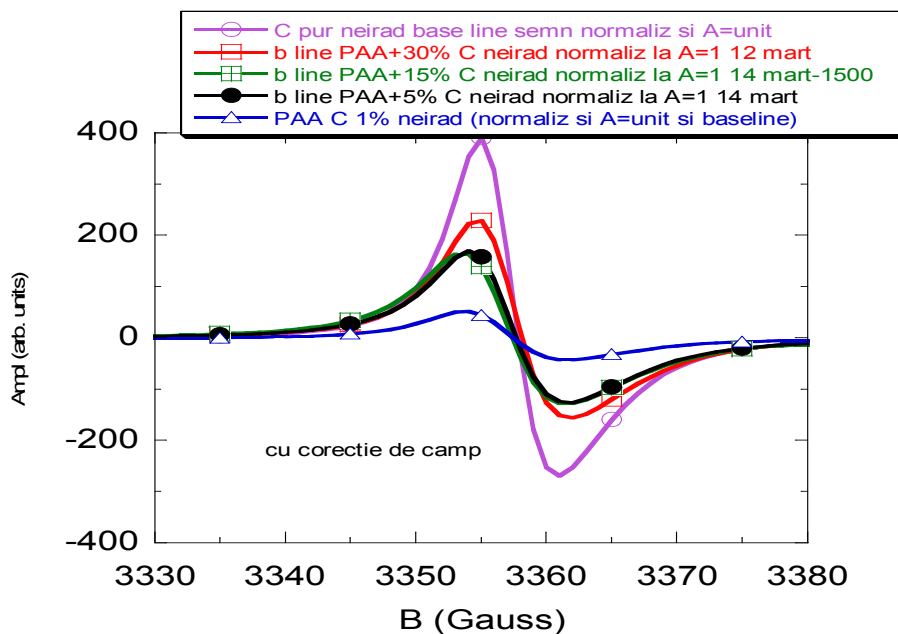


Figure 5.11. The ESR spectra of PAA-Carbon, 1, 5, 15 and 30% pure carbon.

After irradiation, the ESR signal amplitude for pure graphite increases significantly, indicating the emergence of a large number of unpaired electrons, (Fig.5.14.). A similar behaviour is observed for doped samples. For a given concentration of carbon, the ESR signal amplitude compared with the amplitude before irradiation increases. This behaviour is observed over the concentration range of 5% to 30% of graphite in Figure 5.13, but can be observed for all samples. Considering the fact that the signal of pure PAA after irradiation is very small compared to that of graphite, it can be stated that the increase of the EPR signal of the doped samples is mainly determined by graphite.

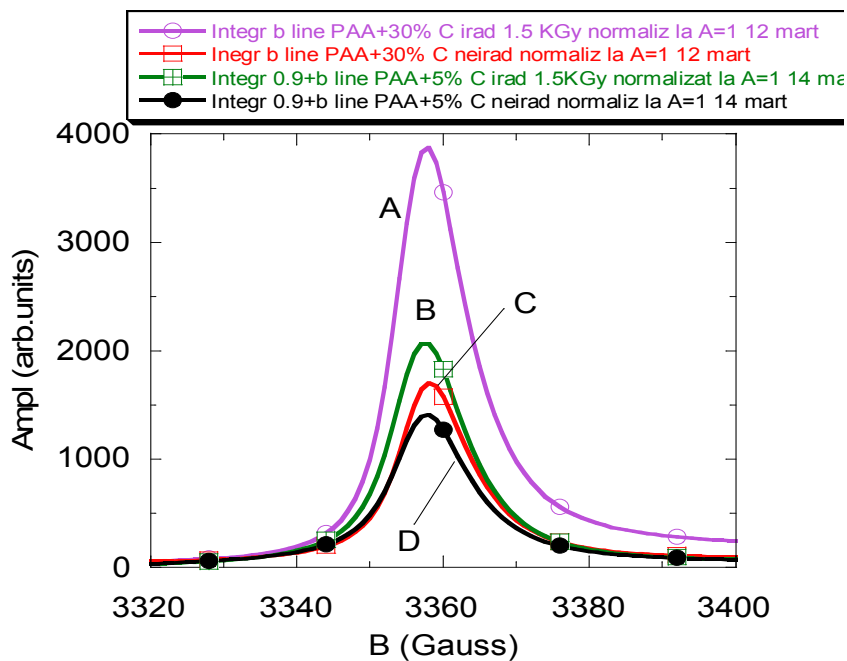


Fig. 5.13. The RES signal absorption of 30% C PAA after irradiation (A), before irradiation (C) and 5% C PAA after irradiation (B) and before irradiation (D).

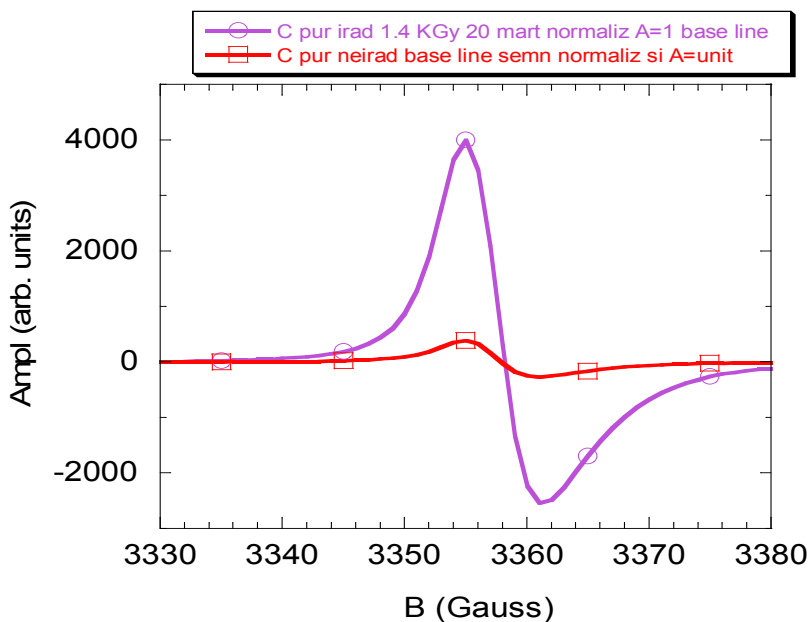


Fig.5.14. The EPR spectrum of pure carbon before and after irradiation.

## 5.2. Spectroscopic Investigation of doped TiO<sub>2</sub> PAA membranes

### 5.2.1. UV-VIS investigations

For pure membranes, the absorbance has a very low value and remains almost constant in the wavelength range of 800-300 nm, but increases in the 300-200 nm range, with a maximum at 207 nm (Fig.5.15.).

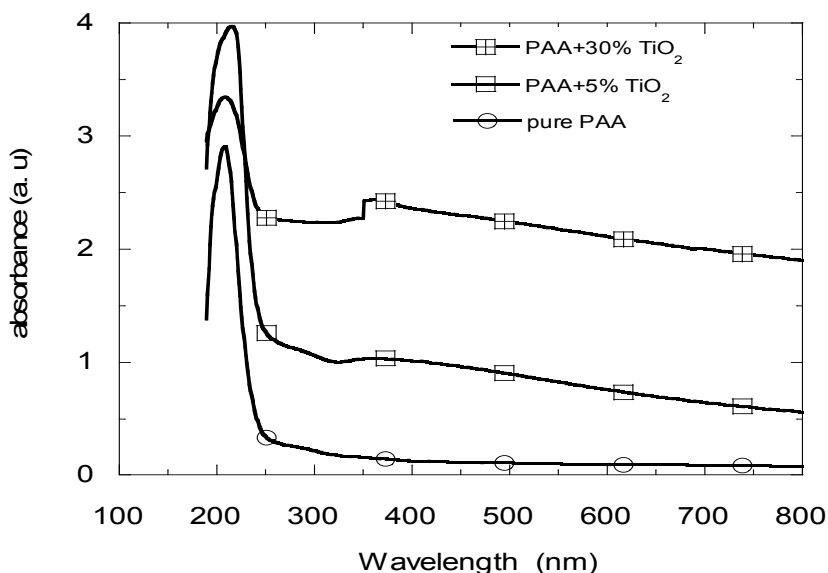


Fig.5.15. The UV-VIS absorption spectra of pure and doped (5 and 30% TiO<sub>2</sub>) PAA membranes.

The presence of a maximum at 207 nm is most likely due to strong absorption of the polymer and the existence of water molecules in the polymer matrix become final after drying the membranes. Knowing the behaviour of water in the UV, we can explain the increased absorption in the 350-200 nm by the existence of a certain quantity of water in PAA membranes.

The UV-VIS absorption is enhanced by the addition of TiO<sub>2</sub>. UV-VIS spectra of composite membranes have the same shape as pure PAA membranes without additional absorption maxima, but the absorbance increases with the amount of TiO<sub>2</sub> continuously throughout the UV-VIS (Fig.5.15.). If the absorbance of the pure membrane remains

almost constant in the 800-300 nm range, the absorbance of the TiO<sub>2</sub> membranes increases slowly but continuously in this area.

### 5.2.2. Raman investigation

The Raman spectra of pure PAA before irradiation are shown in Figure 5.17.

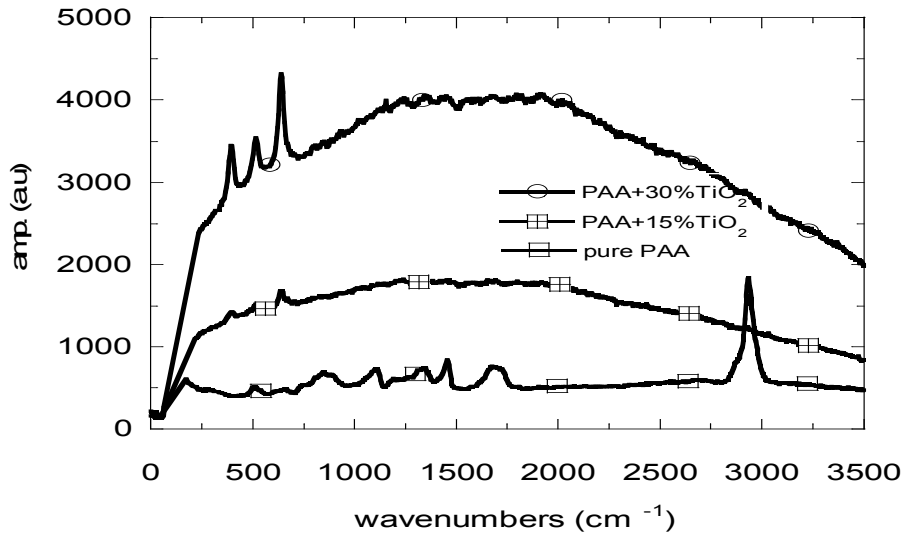


Fig.5.17. The Raman spectra for pure and doped (15 and 30% TiO<sub>2</sub>) irradiated PAA.

The most intense bands of vibration of the polymer are allocated as follows: 500 cm<sup>-1</sup> - COD deformation, 822 cm<sup>-1</sup> - CH<sub>2</sub> twist, 1096 cm<sup>-1</sup> - CH<sub>2</sub>-balancing plan, 1461 cm<sup>-1</sup> - CH<sub>2</sub> deformation, 1690 cm<sup>-1</sup> - C = O stretching.

These bands appear in the spectrum corresponding doped TiO<sub>2</sub> membranes without changes, but with less intensity. In addition, the spectra contain three additional bands at 399 cm<sup>-1</sup>, 513 cm<sup>-1</sup> and 639 cm<sup>-1</sup>. The intensity of these bands increases progressively with the concentration of TiO<sub>2</sub> (Fig.5.17.). TiO<sub>2</sub> has three vibration bands at 400, 514 and 638 cm<sup>-1</sup>, which correspond to the three phases of TiO<sub>2</sub>, rutile, anatase and brooklite. The occurrence of vibration bands of PAA and TiO<sub>2</sub> in the composite material in the same amount of light as pure components suggests that there are no

chemical bonds between the polymer and  $\text{TiO}_2$ . Chemical structure of both components remains unchanged in the composite. After irradiation spectrum of pure PAA membrane does not change significantly. Characteristic bands of the polymer occur at the same numbers as before the radiation beam, the amplitudes are increased slowly to the overall change in shape. They act as samples containing a certain amount of water, (Fig.5.18.).

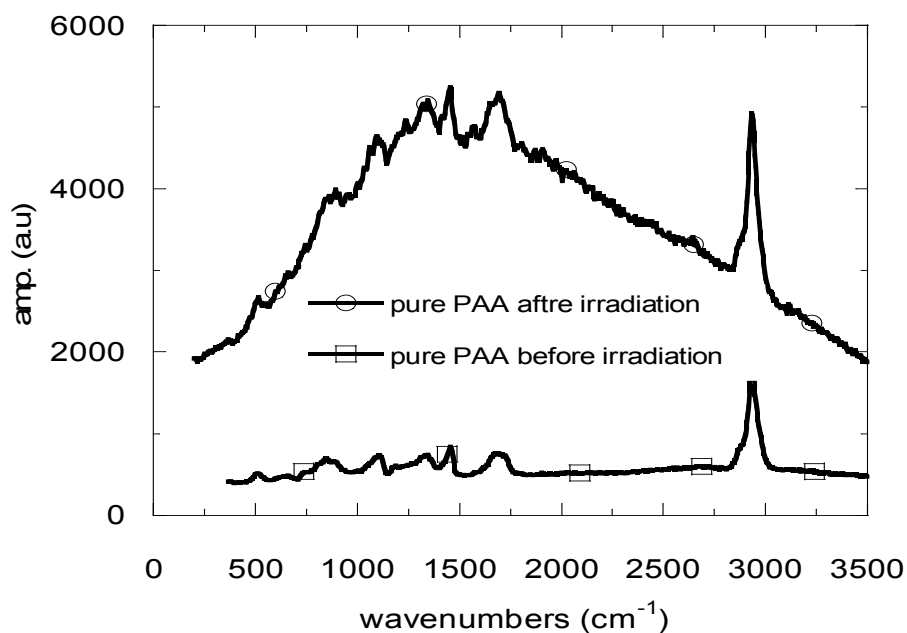


Fig.5.18 The Raman spectra of pure PAA membranes, before and after irradiation.

It is known that aqueous gels made from polymer membranes contain the remaining water in the vacant spaces of the polymer matrix, which remains even after the complete drying. Under gamma irradiation, the polymer matrix is disrupted and allows water to aggregate in areas with a larger size than before irradiation. The Raman spectrum changes its shape and therefore this contribution may be attributed to water.

### General conclusions

The polymers, which have as monomers the polyvinyl alcohol (PVA) and polyacrylic acid (PAA), have many practical applications both in gel form as well as

membranes. Their properties can often be changed after doping with various inorganic substances, thus expanding the range of possible applications of these compounds.

The gamma irradiation also causes changes in the properties of these materials; some of them may be exploited for practical purposes. Electrical and spectroscopic investigations have demonstrated that contamination with inorganic nanoparticles causes changes of mechanical, electrical, optical and crystalline properties, without affecting the fundamental chemical structure of polymers and dopants.

The gamma irradiation has destructive effects on pure polymers that can be attenuated in some cases by contamination with inorganic compounds which are stable to radioactive action. Relaxation, occurred after the removal from the radioactive medium, leads to the return of some parameters to values close to the initial ones (e.g. electric parameters), while other radiation-induced changes, such as the degree of crystallinity of the matrix polymer or architectural changes, are irreversible.

These behaviours can be successfully exploited at producing proton exchange PVA membranes, doped with  $\text{TiO}_2$ , by substituting the complex chemical treatment with a moderate gamma irradiation.

The importance of these materials will significantly increase once the research and the new technology advances will enable their current use in complex pharmaceutical systems as controlled release support of the active substance, or as electrodes and solid electrolytes in proton exchange fuel cells.